THE ELECTRONIC ABSORPTION SPECTRA OF NH_2 AND ND_2

By K. DRESSLER and D. A. RAMSAY

Division of Pure Physics, National Research Council, Ottawa, Canada

(*Communicated by G. Herzberg, F.R.S.—Received* 30 *December* 1958)

[Plates 3 to 5]

CONTENTS

The absorption spectra of $^{14}NH_2$, $^{15}NH_2$ and $^{14}ND_2$ have been photographed in the region 3900 to 8300 Å with a 21 ft. concave grating spectrograph. The radicals are produced by the flash photolysis of $^{14}NH_3$, $^{15}NH_3$ and $^{14}ND_3$ respectively. A detailed study of the $^{14}NH_2$–$^{15}NH_2$ isotope shifts suggests that the molecule has a linear configuration in the excited state and that the spectrum consists of a long progression of the bending vibration in this state. These conclusions have been confirmed by detailed rotational and vibrational analyses of the $^{14}NH_2$ and $^{14}ND_2$ spectra. The spectra consist of type *C* bands for which the transition moment is perpendicular to the plane of the molecule. For NH_2, sixteen bands of the progression $(0, v_2', 0) \leftarrow (0, 0, 0)$ have been identified with $v_2' = 3, 4, \ldots, 18$. In addition four bands of a subsidiary progression $(1, v_2', 0) \leftarrow (0, 0, 0)$ have been found; these bands derive most of their intensity from a Fermi-type resonance between $(0, v_2', 0)$ and $(1, v_2'-4, 0)$ levels in the excited state. The interaction constant W_{ni} is 72 ± 3 cm^{-1}. For ND_2, fourteen bands of the principal progression ($v_2' = 5$ to 18) and one band of the subsidiary progression have been identified. The upper state vibration frequencies $\omega_1^{0'}$ and $\omega_2^{0'}$ are 3325 cm^{-1} and 622 cm^{-1} for NH_2 and 2520 cm^{-1} and 422 cm^{-1} for ND_2 respectively. The bending frequencies are unusually low; moreover, the anharmonicities of the bending vibration are unusually large and negative ($x_{22}^{0'} = 11{\cdot}4$ cm^{-1} for NH_2 and $8{\cdot}1$ cm^{-1} for ND_2). The origin of the system lies in the region of 10000 cm^{-1}.

Ground-state rotational term values have been derived from observed combination differences; values for the rotational constants A_{000}'', B_{000}'' and C_{000}'' and for the centrifugal distortion constants D_A'', D_B'' and D_C'' have been determined. The bond lengths and bond angles for NH_2 and ND_2 agree and are $1{\cdot}024 \pm 0{\cdot}005$ Å and $103° 20' \pm 30'$ respectively. Small spin splittings have been observed.

In the excited state an unusual type of vibronic structure has been found. Successive levels of the bending vibration consist alternately of Σ, Δ, Γ, ... and Π, Φ, ... vibronic sub-levels with large vibronic splittings. The origins of the vibronic sub-bands may be represented by the formula $\nu_0^K = \nu_0 - GK^2$, where G is ~ 27 cm^{-1} for NH_2 and ~ 19 cm^{-1} for ND_2. The rotational levels show both spin and *K*-type doubling. No simple formula has been found to fit the energies of the Π, Δ, Φ and Γ rotational levels; the Σ levels fit the formula $F(N) = BN(N+1) - DN^2(N+1)^2$, though with a negative value for D. By extrapolating the B values for the Σ levels to $v_2' = 0$ we

obtain $B'_{000} = 8{\cdot}7_8$ cm^{-1} for NH_2 and $4{\cdot}4_1$ cm^{-1} for ND_2. These values are consistent with a linear configuration with a bond length of $0{\cdot}97_5$ Å. The significance of this short bond length is discussed.

An explanation of the complex vibronic structure is given. The two combining states are both derived from an electronic Π state which is split by electronic-vibrational coupling for the reasons advanced by Renner. A detailed correlation diagram is given. A quantitative treatment of this effect by Pople & Longuet-Higgins gives good agreement with the experimental data.

1. Introduction

The absorption spectrum of the NH_2 free radical was first observed during flash photolysis experiments with ammonia (Herzberg & Ramsay 1952) and hydrazine (Ramsay 1953). The spectrum extends from approximately 3900 to 8300 Å and consists of a large number of irregularly spaced absorption lines. Many of the absorption lines coincide exactly in wavelength with lines observed in the spectrum emitted by an oxyammonia flame (Herzberg & Ramsay 1952). The identity of the two band systems is thus established. The flame bands, known as the α-bands of ammonia, have been observed in a large variety of sources (see Ramsay 1957*a*, references 8–31) and for a long time have been attributed to the NH_2 free radical. Confirmation of this assignment was afforded by the absorption experiments and by the observation of isotopic shifts when ^{14}N was replaced by ^{15}N and when H was replaced by D (Herzberg & Ramsay 1953). Final proof of the assignment of the band system to NH_2 was derived from the rotational analysis of some of the bands (Ramsay 1956, 1957*b*).

The purpose of this paper is to present the details of the rotational and vibrational analysis of the NH_2 and ND_2 spectra since the analysis affords many features of both spectroscopic and theoretical interest. The spectrum is due to an electronic transition from a ground state in which the molecule is bent and is a highly asymmetric top, to an excited state in which the molecule vibrates about a linear configuration. This is the first example of a detailed analysis of a transition of this kind. The excited state exhibits a previously unobserved and complex pattern of vibronic and rotational energy levels. The vibronic structure of this pattern, together with the polarization and electronic energy of the transition, may be understood (Dressler & Ramsay 1957) if it is assumed that the two combining states are derived from a hypothetical Π state. The vibronic levels of this Π state are assumed to split into two groups, correlating respectively with the vibronic levels observed in the excited state and with vibrational and rotational levels of the ground state. The large splittings observed are due to an interaction between electronic and vibrational motion of the type predicted by Herzberg & Teller (1933) and discussed in detail by Renner (1934). The observed splittings, however, are much larger than those considered by Renner and have been explained quantitatively in a recent theoretical paper by Pople & Longuet-Higgins (1958).

2. Experimental

The absorption spectra used in the present analysis were obtained by the flash photolysis of ammonia using the 'microsecond' flash photolysis apparatus described in an earlier publication (Callomon & Ramsay 1957). The quartz reaction cell was 50 cm long and was fitted with a system of multiple reflexion mirrors of the type described by White (1942) and Bernstein & Herzberg (1948). The mirrors were coated with silver for the

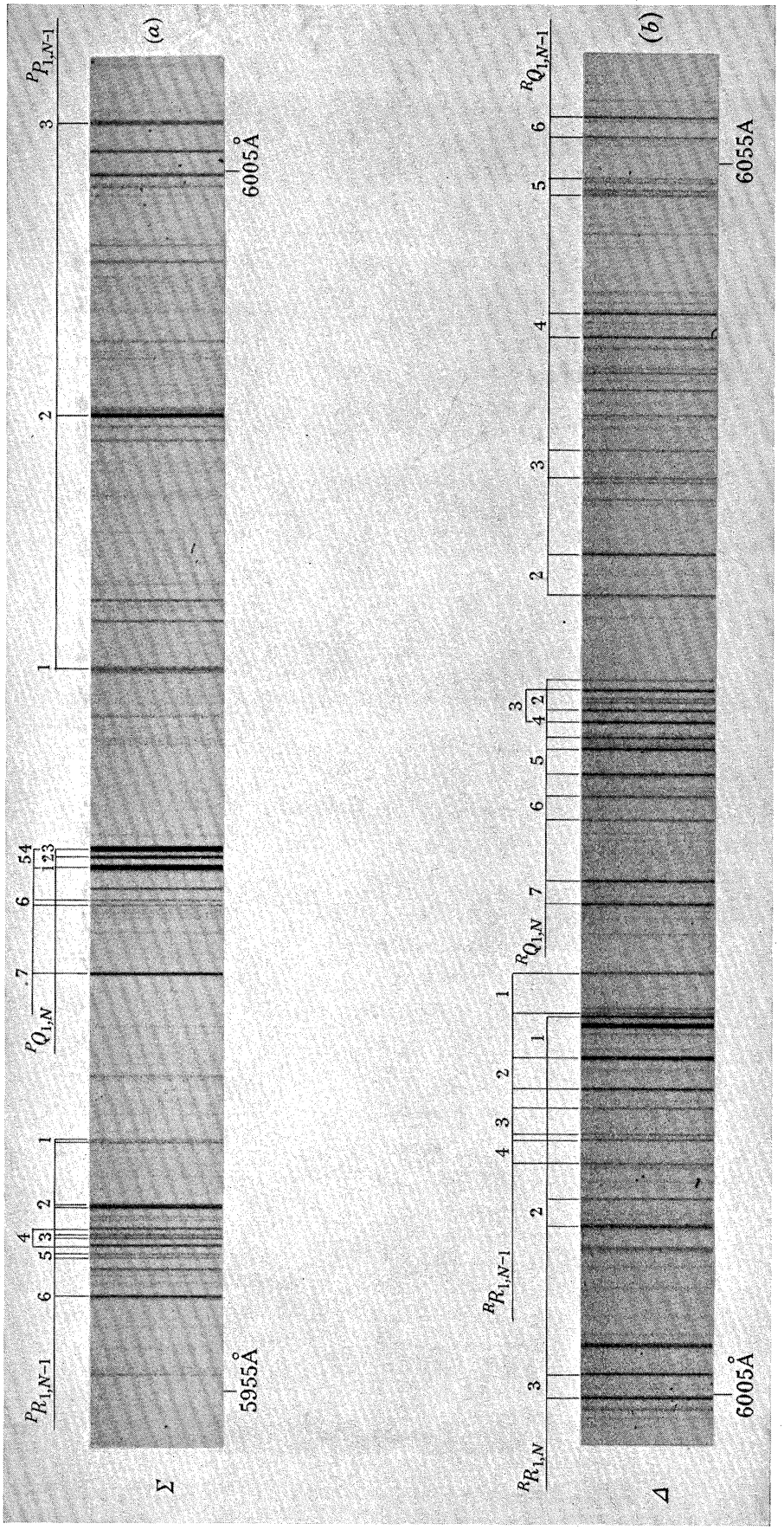

FIGURE 1. Rotational assignments for the $(0, 9, 0) \leftarrow (0, 0, 0)$ band of NH_2. In (*a*) the three branches of the Σ vibronic sub-band are shown. The strong Q branch 'doublet' is the strongest feature in the absorption spectrum of NH_2. A rotational perturbation may be seen in the R branch. In (*b*) the strongest R and Q branches of the Δ vibronic sub-band are shown.

(*Facing p.* 554)

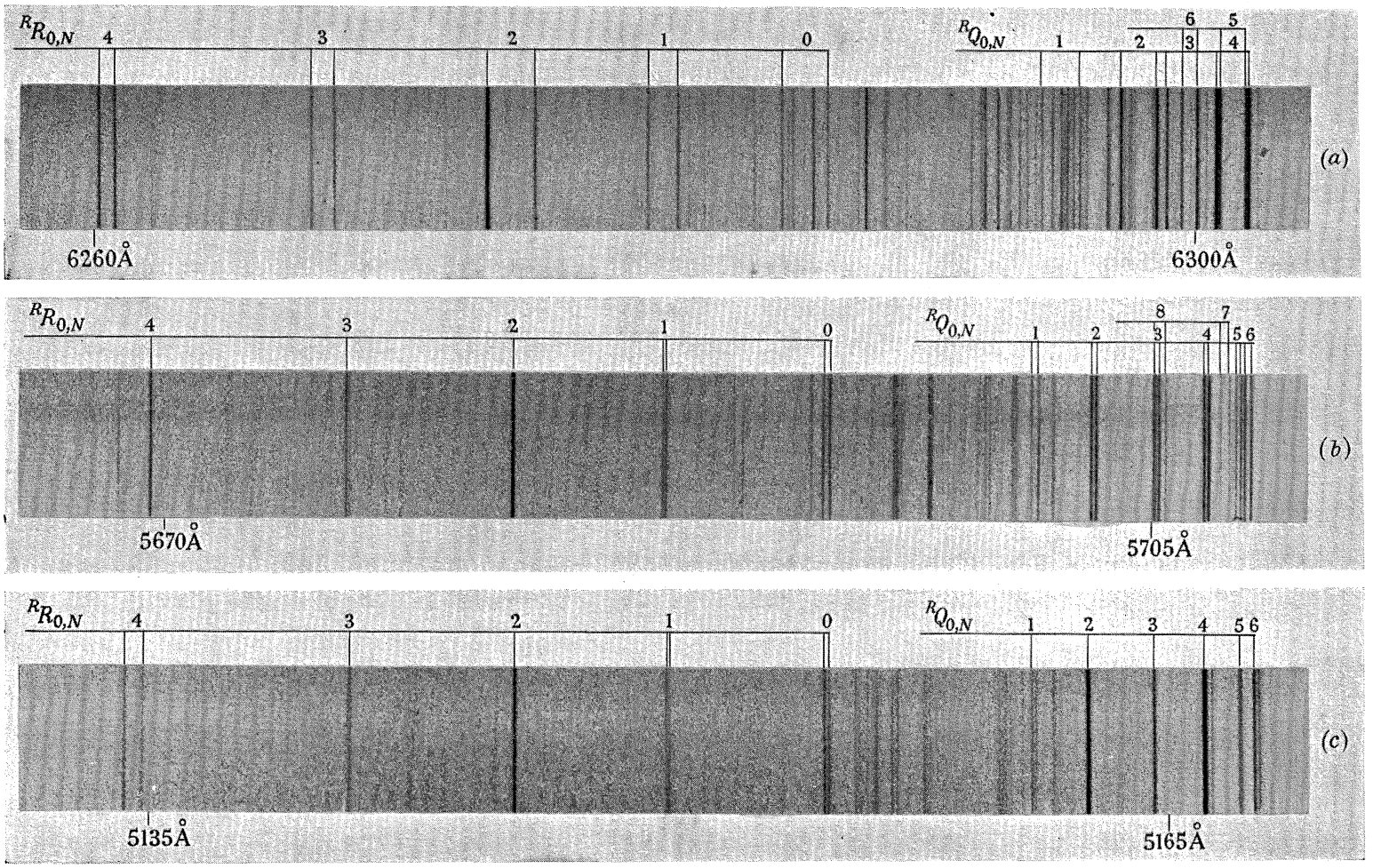

FIGURE 2. Comparison of the strong R and Q branches in the Π vibronic sub-bands of (a) the (0, 8, 0) ← (0, 0, 0) band, (b) the (0, 10, 0) ← (0, 0, 0) band and (c) the (0, 12, 0) ← (0, 0, 0) band of NH_2. The decrease in spin splitting from (a) to (b) to (c) may be noted. A rotational perturbation may be seen in the $R(4)$ line in (c).

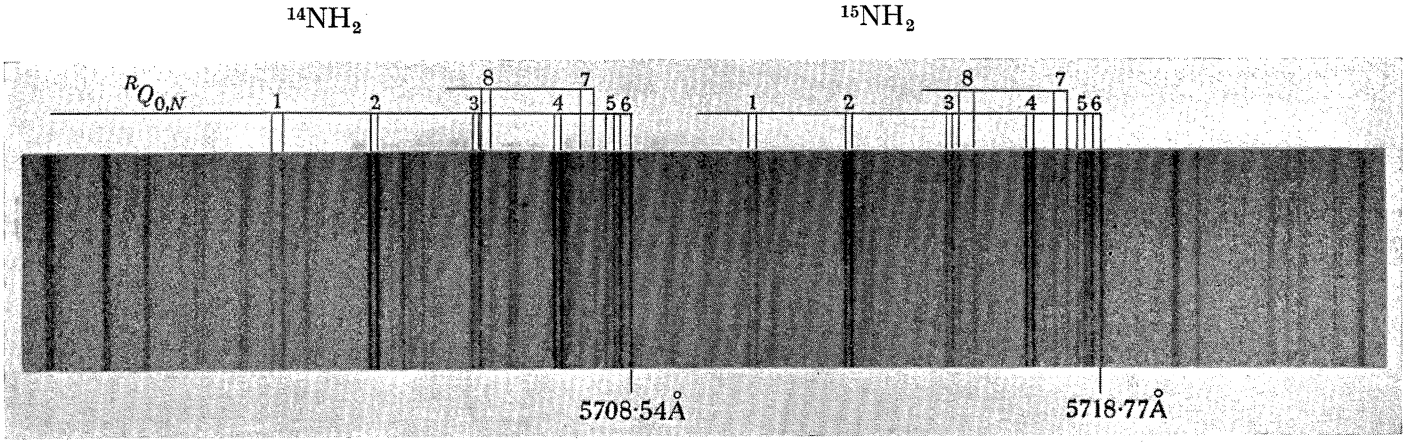

FIGURE 3. $^{14}NH_2$–$^{15}NH_2$ isotope shifts in the strong Q branch of the (0, 10, 0) ← (0, 0, 0) band of NH_2. This spectrogram was obtained by the flash photolysis of a mixture of $^{14}NH_3$ and $^{15}NH_3$ in roughly equal proportions.

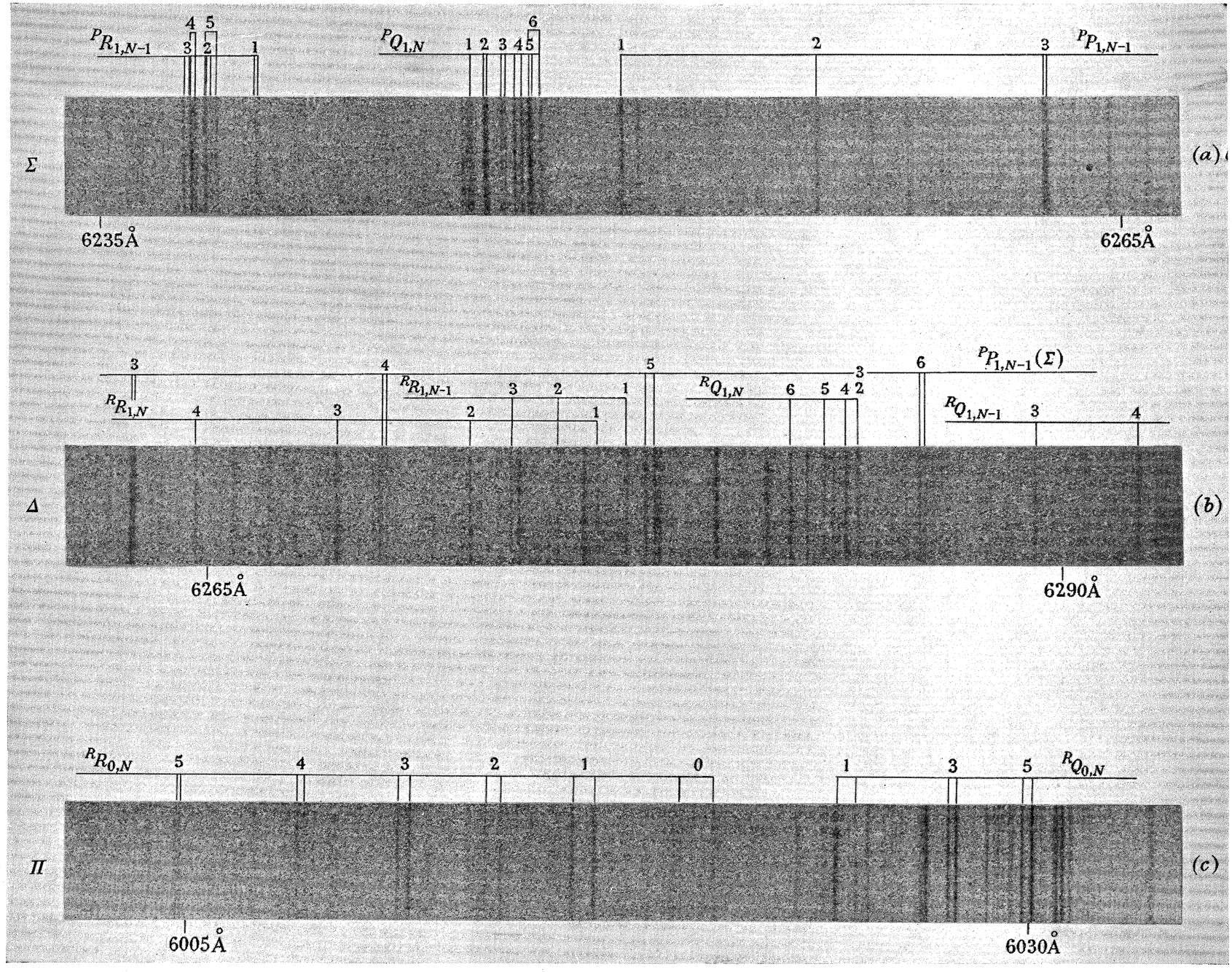

FIGURE 4. Rotational assignments for the strongest bands in the absorption spectrum of ND_2. In (*a*) the three branches of the Σ vibronic sub-band of the (0, 11, 0) ← (0, 0, 0) band are shown. In (*b*) the strongest *R* and *Q* branches of the Δ vibronic sub-band of the same band are given, together with the overlapping *P* branch from the Σ vibronic sub-band. In (*c*) the strong *R* and *Q* branches of the Π vibronic sub-band of the (0, 12, 0) ← (0, 0, 0) band are shown.

region 4000 to 9000 Å and with aluminium for the region below 4000 Å. The photolysis flash lamp was 25 cm long and was fired by a 40 μF, 7 kV condenser. The duration of the photolysis flash was ~ 20 μs. Absorption spectra were photographed using a quartz capillary flash lamp which was fired by a 2 μF, 10 kV condenser. The duration of the 'source' flash was ~ 10 μs. The time interval between the photolysis and the 'source' flashes was controlled by a delay circuit and was ~ 25 μsec. The precise value of the delay was not important since the half-life of the NH_2 radicals was found to be ~ 100 μs. Spectra were photographed in the region 2200 to 9000 Å using the various orders of a 21 ft. concave grating spectrograph; Eastman Kodak I–O, I–F and hypersensitized I–N plates were used.

Absorption bands of NH_2 were found in the region 3900 to 8300 Å. The intensity of the bands was found to be a maximum using a pressure of ammonia of 1 to 3 mm Hg and no added inert gas. Final plates were therefore taken under these conditions, the sample of gas being changed between flashes. Twelve traversals of the mirror system were used. The number of flashes required to give satisfactory exposures varied from 60 to 100 depending on the spectral region. Reproductions of five of the stronger regions of the NH_2 spectrum are shown in figures 1 and 2, plates 3 and 4.

The absorption spectra of $^{15}NH_2$ and of $^{14}ND_2$ were also investigated. The starting materials were a sample of ammonia containing 50% $^{15}NH_3$ and a sample of ND_3 obtained by the action of 99% D_2O on Ca_3N_2. The isotope shifts between corresponding $^{14}NH_2$ and $^{15}NH_2$ lines could in most cases be established by inspection and are shown in figure 3, plate 4, for a small region of the spectrum involving the 5708 Å band. No such correlation however was obvious between the $^{14}NH_2$ and $^{14}ND_2$ lines. Three of the stronger regions in the absorption spectrum of ND_2 are shown in figure 4, plate 5.

The spectrum of an iron arc was used for wavelength calibration. The NH_2 and ND_2 plates were measured four times but no extensive measurements were carried out on the $^{15}NH_2$ plates. The wavelengths of the comparison lines were taken from the M.I.T. wavelength tables (Harrison 1939) and the vacuum corrections of Edlén (1953) were used. The vacuum wave numbers of the NH_2 and ND_2 lines which have been assigned are given in tables 1 and 2† respectively, together with the rotational and vibrational assignments of these lines. A complete list of all the measured NH_2 lines will be given in a separate communication. The relative accuracy of the measurements of the sharp lines is $\sim 0{\cdot}02$ cm^{-1}. The only measurements which were carried out on the $^{15}NH_2$ plates involved the measurement of the $^{14}NH_2$–$^{15}NH_2$ isotope shifts of some of the stronger lines. About 250 of these shifts were measured throughout the spectrum with an accuracy of $\sim 0{\cdot}1$ cm^{-1}.

3. Preliminary analysis; $^{14}NH_2$–$^{15}NH_2$ isotope shifts

One of the puzzling features of the NH_2 spectrum is that there is no obvious similarity between the rotational structure in any region of the spectrum and that of any other region, with one exception. This exception involves two bands in the region of 5708 and 5166 Å where the similarity in rotational structure is quite marked (see figure 2*b*, *c*); it is not obvious, however, why certain lines should appear as doublets in the one band and as singlets in the other. These two bands are separated by 1834 cm^{-1}, an interval which

† The tables appear at the end of the paper.

cannot immediately be correlated with any vibration frequency in the upper or lower state. It is now known that this interval corresponds to a double quantum of the bending frequency in the excited state. Initial attempts to find further bands with similar rotational structure on either side of the 5708 and 5166 Å bands were not successful, though such bands have now been identified at 6299 and 4720 Å. The reasons for the failure of the initial attempts are (*a*) the large variation in the doublet splittings of the rotational lines from band to band (see figure 2*a*), and (*b*) the rather large *increase* in vibrational interval with increasing quantum number of the bending vibration.

The main clue to the whole analysis lay in a detailed study of the isotope shifts between the $^{14}NH_2$ and $^{15}NH_2$ spectra. The $^{14}ND_2$ spectrum was found to be of little assistance in the early analysis since the isotope shifts between the corresponding bands of $^{14}NH_2$ and $^{14}ND_2$ are so large that no obvious correlation was possible. For the $^{14}NH_2$ and $^{15}NH_2$

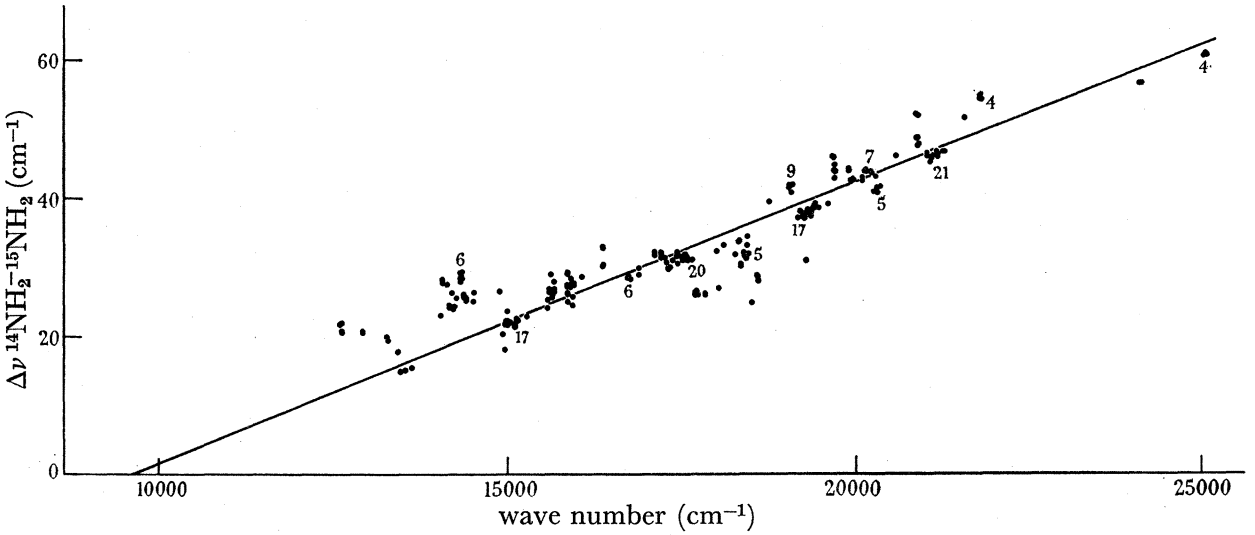

FIGURE 5. $^{14}NH_2$–$^{15}NH_2$ isotope shifts plotted against the wave numbers of the $^{14}NH_2$ lines. The small numbers indicate the number of overlapping points. Intercept = 9600 cm^{-1}; slope = 0·00407.

spectra the isotope shifts are much smaller; the shifts vary from 15 cm^{-1} at the long wavelength end of the spectrum to 60 cm^{-1} at the short wavelength end. The isotope shifts of 250 of the stronger lines are shown in figure 5 plotted against the wave numbers of the $^{14}NH_2$ lines. The points lie fairly close to a straight line with an intercept of 9600 cm^{-1} and a slope of 0·00407. The transition thus involves a low-lying excited state.

The value of the slope, namely 0·00407, turned out to be very significant, since from this number it was possible to deduce that in the excited state the equilibrium configuration is very probably linear. It was initially assumed, and later confirmed, that the strong lines in the absorption spectrum originate in the (0, 0, 0) vibrational level of the ground state. The change in the $^{14}NH_2$–$^{15}NH_2$ isotope shift throughout the spectrum is thus due primarily to the change in the vibrational quantum numbers in the excited state, though a small contribution to the isotope shift will result from the rotation of the molecule. The principal factors determining the ratio of the isotope shift $\Delta\nu$ to the vibrational frequency ν in the excited state are (i) the nuclear masses, (ii) the H—N—H angle,

and (iii) the particular vibration excited, i.e. ν_1, ν_2 or ν_3. The value of $\Delta\nu/\nu$ will also depend to some extent on the force constants in the excited state but this effect is of secondary importance. Initially it was assumed that the vibrations are harmonic and that the N—H stretching and H—N—H bending force constants are similar to those for the ground state of ammonia, namely $k_1 = 6{\cdot}0\times10^5$ dyn/cm and $k_\delta/l^2 = 0{\cdot}6\times10^5$ dyn/cm (Herzberg 1945, p. 177). The values of $\Delta\nu/\nu$ were calculated and are given in table 3 as a function of the apex angle and of the particular vibration involved. For comparison purposes the corresponding values obtained from the final set of force constants are also given. It is seen that the observed value of $\Delta\nu/\nu$ cannot be explained for any value of the apex angle on the assumption that a progression of the symmetrical stretching vibration ν_1 is excited. (It was later found that some of the *weaker* bands involve the excitation of one quantum of this vibration.) The observed value can only be explained if it is assumed that the molecule is linear, or nearly linear in the excited state, and that the spectrum involves a progression of ν_2 or ν_3 or of both of these vibrations. According to a selection rule given by Herzberg & Teller (1933) the antisymmetric vibration, ν_3, may only be excited in double quanta, and furthermore the intensity should decrease very rapidly with increasing vibrational quantum number. One is therefore led to the conclusion that the apex angle in the excited state is close to 180°, and that the spectrum consists principally of a long progression of ν_2. We shall see that both of these conclusions prove to be justified.

4. Rotational analysis; Σ and Π sub-bands

Since it was not possible initially to identify the various bands of the NH_2 spectrum and their rotational branches, it was found necessary to calculate various trial spectra and to compare the calculated spectra with the observed data. In the initial calculations it was assumed that the molecule is linear in the excited state as suggested above, and non-linear in the ground state. In both states the N—H bond length was assumed to be the same as in the ammonia molecule.

The H—N—H angle in the ground state was estimated from the length of the progression of the bending vibration by application of the Franck–Condon principle as follows. The origin of the progression lies at ~ 9600 cm^{-1}, whereas the strongest bands appear in the region 16000 to 17000 cm^{-1}. The difference $\Delta\theta$ between the equilibrium angles of the upper and lower states may therefore be estimated from the equation $\frac{1}{2}k_\delta\Delta\theta^2 = hc\Delta\nu$, where $\Delta\nu \sim 7000$ cm^{-1}. By interpreting the interval of 1834 cm^{-1} between the 5708 and 5166 Å bands as a double quantum of ν_2, the bending force constant was found to be $k_\delta = 2{\cdot}3\times10^{-12}$ dyn cm/rad. In this way $\Delta\theta$ was found to be $\sim 70°$. These calculations suggest therefore that the ground state is a highly asymmetric top with an H—N—H angle in the region of 110°.

The rotational energy levels of the ground state were designated by the usual 'double K' notation $N_{K_a,\,K_c}$, where N is the quantum number of the resultant angular momentum excluding electron spin. It was found convenient to use the same notation for the excited state. In the excited state K_a is a good quantum number and will be simply referred to as K'; in the ground state the corresponding quantum number is not in general a good quantum number though for the purposes of the interpretation of the spectrum it has been found convenient to denote it by K''. Trial sets of energy levels for the ground state

were calculated using the method of King, Hainer & Cross (1943), assuming various values for the H—N—H angle in the region of 110°. Rotational energy levels for the upper state were calculated using the simple formula $F(N) = BN(N+1)$. The effects of spin doubling and of centrifugal distortion were neglected in the initial calculations.

The selection rules were deduced from the theoretical considerations given in § 7. According to these arguments the observed spectrum should correspond to the allowed transition $^2A_1 \leftarrow {}^2B_1$ for which the transition moment is perpendicular to the plane of the molecule. The spectrum should therefore consist of type C bands for which the rotational selection rules are (Herzberg 1945, p. 468)

$$\Delta J = 0, \pm 1; \quad J = 0 \quad \not\leftrightarrow J = 0, \tag{1}$$

$$+ + \leftrightarrow + - \quad \text{and} \quad - - \leftrightarrow - +. \tag{2}$$

An estimate of the relative intensities of the various rotational transitions was obtained by the method of Cross, Hainer & King (1944) using a 'mean κ' for the upper and lower states and assuming a room temperature distribution of ground-state rotational energy levels. The deviations to be expected from the intensities calculated by this method, due to the difference in κ for the upper and lower states, have been discussed by Allen (1954). Since the NH_2 molecule has a twofold axis of symmetry, the overall symmetry of the rotational levels will be either symmetric or antisymmetric with respect to a rotation by 180° about this axis. The symmetry properties of the rotational eigenfunctions have been given by Dennison (1931). If we assume that the electronic symmetry species of the lower and upper states are B_1 and A_1 respectively (see § 7), the overall symmetry properties for levels involving totally symmetric vibrations are readily obtained. The H nuclei follow Fermi statistics and the ratio of the number of NH_2 molecules in the symmetric to antisymmetric rotational levels is 1:3 respectively. An alternation in the intensities of successive rotational lines in all branches is therefore to be expected. Since D nuclei follow Bose statistics the corresponding ratio for ND_2 is 2:1.

Trial spectra were calculated on the basis of the above assumptions and attempts were made to fit the calculated spectra to the observed data. The rotational lines of the calculated spectra were grouped into branches in a manner similar to that of Cross *et al.* (1944) except that the ${}^{ce}R_{1,0}$, ${}^{ce}P_{\bar{1},0}$, ${}^{co}R_{1,0}$ and ${}^{co}P_{\bar{1},0}$ branches were sorted in terms of K'_a rather than K'_c. Moreover, it was found convenient to distinguish between the branches which have different values of K'_a but which have the same symbol on the Cross *et al.* notation. The most general notation which would distinguish the various possible branches, including the components of the spin doublets, would be of the form

$${}^{c,\Delta K_a,\Delta K_c}\Delta J(J_{K_a,K_c}).$$

For the present problem, however, it was found convenient to denote the branches by the abbreviated form of notation

$${}^{\Delta K_a}\Delta N_{K_a,K_c},$$

where no distinction is made between the components of the spin doublets.

Since the bands near 5708 and 5166 Å appeared to have the simplest rotational structures, attempts were made to interpret these bands first. In each of the bands two branches are readily recognized, and the alternation in the intensities of successive

rotational lines is clearly seen (see figure 2*b*, *c*). The closely spaced groups of strong lines were initially assumed to be Q branches and the more widely spaced series of lines to shorter wavelengths were assumed to be R branches. According to the calculations there should be two types of strong Q branches, namely ${}^{P}Q_{1,N}$ and ${}^{R}Q_{0,N}$ with associated R branches to shorter wavelengths. The combination differences which may be formed from a ${}^{P}Q_{1,N}$ branch and its associated ${}^{P}R_{1,N-1}$ branch refer to the lower state (see figure 6), while the differences formed from a ${}^{R}Q_{0,N}$ branch and its associated ${}^{R}R_{0,N}$ branch refer to the upper state (see figure 7). The differences which can be formed between the Q and

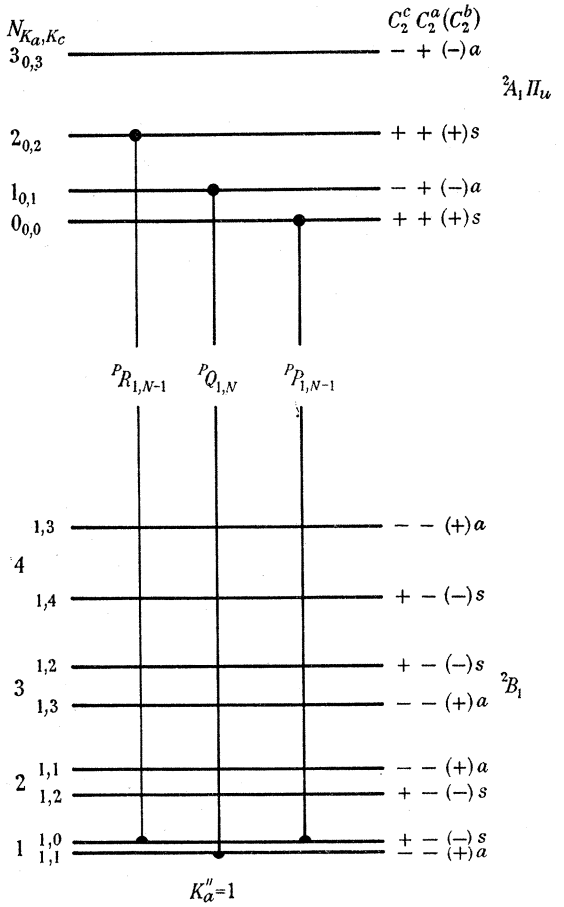

FIGURE 6. Energy level diagram for the first lines of the Σ vibronic sub-bands of NH_2.

R branches of the 5708 Å band do not agree with the corresponding differences for the 5166 Å band, hence the Q branches cannot be of the type ${}^{P}Q_{1,N}$. If the Q branches are of the type ${}^{R}Q_{0,N}$ then the calculations show that there should be two further branches, namely ${}^{P}Q_{2,N-1}$ and ${}^{P}P_{2,N-1}$ (see figure 7), such that the upper-state combination differences which can be formed between these new branches are the same as those which can be formed between the ${}^{R}Q_{0,N}$ and ${}^{R}R_{0,N}$ branches, i.e.

$$ {}^{R}R(N)-{}^{R}Q(N) = {}^{P}Q(N+1)-{}^{P}P(N+1). \tag{3} $$

These branches were identified in the 5708 and 5166 Å bands and the upper-state combination differences were found to check satisfactorily within each band. In cases where the P, Q and R lines appear as doublets, the combination differences were formed

separately between the higher and the lower wavelength components. Lower-state combination differences were next formed in the following manner:

$$^{R}R(N)-{}^{P}Q(N+1) = {}^{R}Q(N)-{}^{P}P(N+1). \tag{4}$$

These lower-state combination differences were found to check satisfactorily between the 5708 and 5166 Å bands, thus providing strong support for the validity of the assignments.

The four branches which have been identified so far all involve upper-state rotational levels with $K' = 1$. According to the calculations there should be nine branches which involve levels with $K' = 1$ and for which $\Delta K_a = \pm 1$ (see figure 7). All nine branches

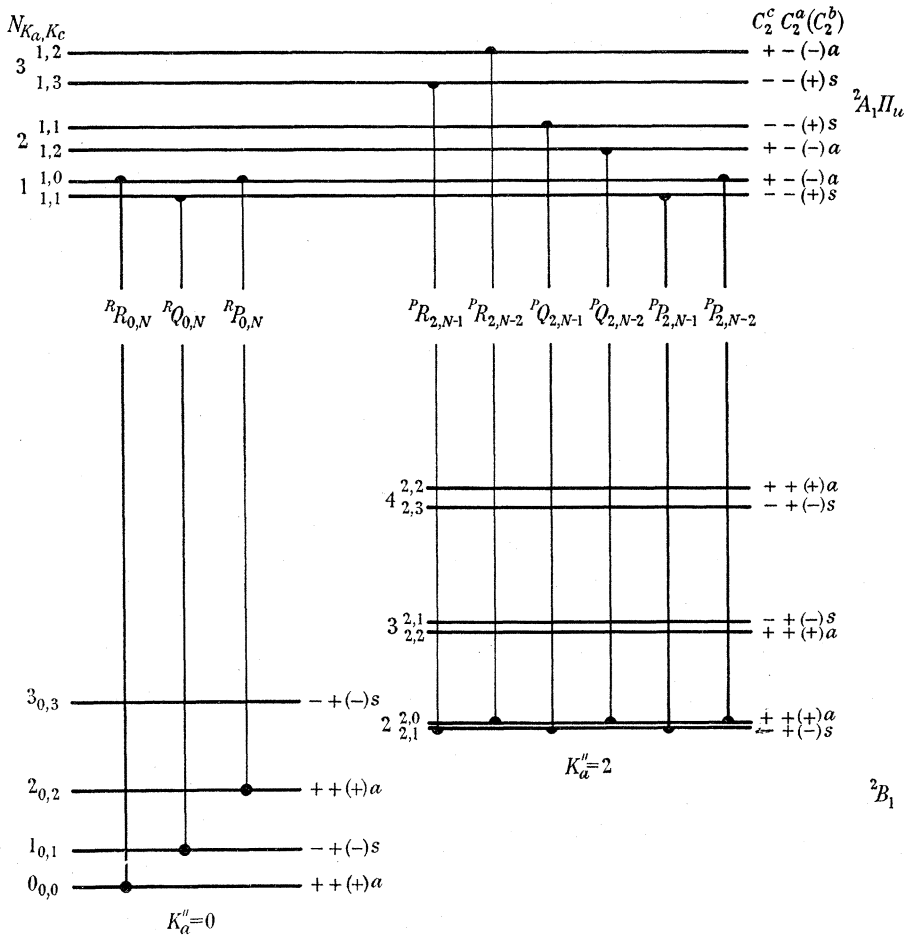

FIGURE 7. Energy level diagram for the first lines of the Π vibronic sub-bands of NH_2.

have now been found (see table 1), although in some of the weaker branches only one or two lines have been identified. The assignments have all been checked by means of upper- and lower-state combination differences. From the type C selection rules (1) and (2) it is found that other branches with $\Delta K_a = -3, -5, \ldots$ are permitted although, according to the intensity calculations of Cross *et al.* (1944), these branches will be extremely weak. Indeed no branches of this kind have yet been found. The nine observed branches with $K' = 1$ constitute a sub-band which we shall refer to as a Π vibronic sub-band.

With the ground-state combination differences obtained from these two bands attempts were made to find other bands with similar rotational structures in other regions of the spectrum. Such bands were found in the regions of 6967, 6299, 4720 and 3995 Å. The rotational assignments for these bands are given in table 1. It may be noted that the spacings of the spin doublets in these bands are considerably larger than in the 5708 and 5166 Å bands (see figure 2) and this accounts for the greater difficulty in recognizing the various branches of the bands. There are presumably two further bands of the same type in the regions of 7750 and 4335 Å, but although several absorption lines have been observed in these regions, it has not been possible to make unambiguous assignments. The ground-state combination differences obtained from all the observed Π vibronic sub-bands agree with each other within the accuracy of the measurements and provide striking support for the validity of the assignments. A typical set of ground-state combination differences is given in table 4B. It may be noted that the values obtained from the high-frequency components of the spin doublets are slightly different from the values obtained using the low-frequency components. The differences between the two sets of values is due to a small but measurable spin splitting of the ground-state rotational levels. It may be noted also that the order of the observed differences at the violet end of the spectrum is the reverse of the order observed at the red end of the spectrum. This may be attributed to a reversal in the sign of the spin splitting in the upper state for bands at the violet end compared to bands at the red end of the spectrum.

As mentioned above, the calculations predicted that there should be two types of strong Q branches, namely ${}^{P}Q_{1,N}$ and ${}^{R}Q_{0,N}$, of which the latter type has been identified in the Π vibronic sub-bands. Bands with the former type of Q branch involve levels in the upper state with $K' = 0$. According to the calculations there should be only three branches involving levels with $K' = 0$ and for which $\Delta K_a = \pm 1$, namely ${}^{P}R_{1,N-1}$, ${}^{P}Q_{1,N}$ and ${}^{P}P_{1,N-1}$ (see figure 6). Other branches with $\Delta K_a = -3, -5, \ldots$ are permitted by the selection rules, but according to the intensity calculations such branches will be extremely weak compared to the branches for which $\Delta K_a = -1$. The branches which involve levels with $K' = 0$ constitute a sub-band which we shall refer to as a Σ vibronic sub-band. Bands with this type of vibronic sub-band have been found in spectral regions lying approximately midway between the bands with Π vibronic sub-bands, i.e. in the regions of 8154, 7350, 6621, 5977, 5428, 4926, 4511 and 4153 Å. The sub-bands were found to consist of the three branches predicted above; the rotational assignments are given in table 1. The lower-state combination differences obtained from these various bands agree within the accuracy of the measurements, thus providing strong confirmation of the validity of the assignments and showing that the bands originate in the same lower-state vibrational level. Some typical differences are given in table 4A.

The complex NH_2 spectrum has so far been split up into a series of sixteen regularly spaced bands, eight involving Σ vibronic sub-bands and eight involving Π vibronic sub-bands. These sixteen bands form a long progression originating in the ground state of the molecule and involving successive quanta of the bending vibration in the upper state. In a similar manner the ND_2 absorption spectrum was split up into a long progression of bands involving alternately Σ and Π vibronic sub-bands. The rotational assignments for these sub-bands are given in table 2. The lower-state combination differences were again

found to check satisfactorily in alternate bands of the progression. The fact that the vibronic symmetry alternates between Σ and Π for successive bands in both the NH_2 and ND_2 progressions provides very powerful evidence that NH_2 (or ND_2) behaves like a linear molecule in the excited state (see § 5).

5. Vibronic structure; rotational analysis of Δ, Φ, ... sub-bands

It is well known (Herzberg 1945, p. 128) that the bending vibration of a linear triatomic molecule is doubly degenerate and produces an angular momentum $lh/2\pi$ about the internuclear axis. If v_2 quanta of the bending vibration are excited, the quantum number l takes the values $v_2, v_2-2, v_2-4, \ldots, 1$ or 0 depending on whether v_2 is odd or even. For a linear symmetric XY_2 molecule in a totally symmetric electronic state, levels with $l = 0, 1, 2, \ldots$ correspond to Σ_g^+, Π_u, Δ_g, ... vibronic states. The vibronic symmetries of the first few levels of the bending vibration are successively Σ_g^+; Π_u; Σ_g^+, Δ_g; Π_u, Φ_u; Σ_g^+, Δ_g, Γ_g; ..., i.e. the vibronic symmetries alternate between even and odd l values for successive quanta of the bending vibration. Levels with the same value of v_2 but different values of l have the same energy for an harmonic force field. A splitting of the l-degeneracy is produced, however, by higher terms in the potential function, so that the vibrationa energy may be written

$$G(v_1, v_2, v_3, l) = G(v_1, v_2, v_3, 0) + gl^2. \qquad (5)$$

In those molecules where the effects of l-type splitting have been studied experimentally, e.g. CO_2, HCN, N_2O, the quadratic nature of the splitting has been confirmed and the values of g have been found to be of the order of a few cm^{-1}.

In the NH_2 bands described above in which the Σ vibronic sub-bands have been identified, attempts were made to identify Δ, Γ and higher vibronic components. Initially it was assumed that (i) the B-values for the Δ, Γ, ... levels are the same as for the Σ levels and (ii) the value of g in equation (5) is of the order of a few cm^{-1}. These attempts, however, were unsuccessful.

The Δ vibronic sub-bands were eventually identified with groups of lines lying approximately 150 cm^{-1} to *lower* frequencies than the corresponding Σ vibronic sub-bands. According to the selection rules (1) and (2) the Δ sub-bands should consist of twelve principal branches, i.e. branches for which $\Delta K_a = \pm 1$. An energy level diagram is given in figure 8. Of these twelve possible branches, ten have been found and the calculations indicate that the remaining two branches should be weak. The rotational assignments are given in table 1. The lower-state combination differences check satisfactorily between the various bands, and moreover many of the differences are identical with differences obtained from the Σ vibronic sub-bands. It should be pointed out that the lowest value of N' observed in the various branches was $N' = 2$, thus providing very strong evidence that the sub-band is indeed a Δ vibronic sub-band.

The Γ sub-bands were next identified with groups of lines lying approximately 500 cm^{-1} to *lower* frequencies than the corresponding Σ vibronic sub-bands. Again the Γ sub-bands should consist of twelve principal branches subject to the condition $\Delta K_a = \pm 1$, although the intensity calculations indicate that many of these branches should be weak. Only four branches have so far been identified, these branches corresponding to the four strongest branches predicted by the intensity calculations. The assignments are given in table 1.

It may be noted that the lowest value of N' involved in the various branches is $N' = 4$, thus confirming the identity of the sub-band. Furthermore, the branches are very short and no line has so far been identified with $N' > 6$.

According to the calculations it should be possible to observe one or two lines of the I sub-bands ($K' = 6$). It is very difficult to make definite assignments of such lines, however, owing to the scarcity of pairs of lines giving lower-state combination differences.

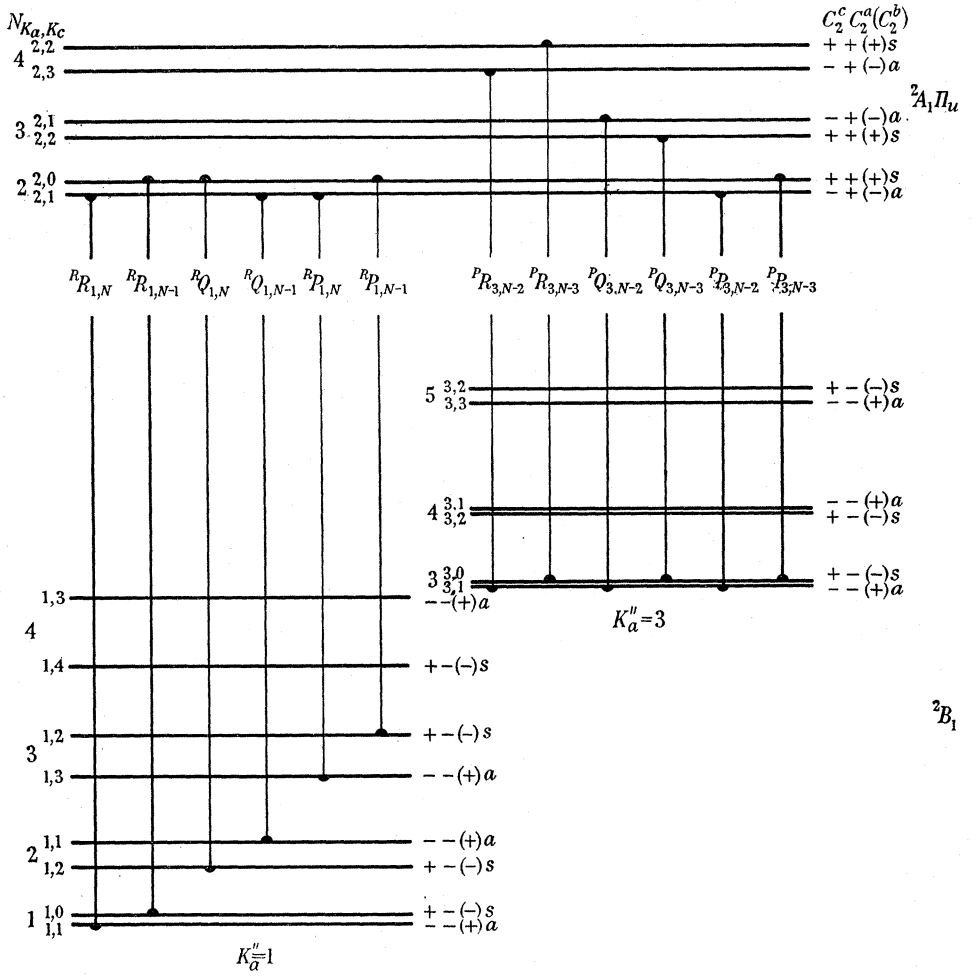

FIGURE 8. Energy level diagram for the first lines of the Δ vibronic sub-bands of NH_2.

Moreover, there is a considerable uncertainty as to the region where such lines should occur owing to the large sub-band splittings. It may be noted that the separations between the Σ, Δ and Γ vibronic sub-bands obey an approximate quadratic law, i.e. the origins of the sub-bands are given by the empirical equation

$$\nu_0^{K'} = \nu_0 - GK'^2, \tag{6}$$

where G is ~ 25 to $30\ cm^{-1}$ (see table 10). If this equation still holds when $K' = 6$ then the I vibronic sub-bands should be displaced by approximately $1000\ cm^{-1}$ relative to the Σ vibronic sub-bands. Although unassigned lines are frequently observed in these spectral regions, it has not been possible to assign any of these lines unambiguously to transitions involved in I vibronic sub-bands. For sufficiently high values of v_2', it should be possible

to observe sub-bands with still higher values of K'. From the intensity calculations, however, it is extremely doubtful if there are any lines of appreciable intensity in the present absorption spectrum belonging to such sub-bands.

The Φ vibronic sub-bands were next identified and were found to lie approximately 300 cm^{-1} to lower frequencies than the corresponding Π sub-bands, in agreement with the predictions made from equation (6). The Φ vibronic sub-bands should consist of twelve principal branches of which the eight strongest branches have been found. The rotational assignments are given in table 1. Again it was noted that the lowest value of N' involved in the various branches was $N' = 3$ in agreement with the assignment of the branches to a Φ vibronic sub-band. Attempts were also made to identify lines belonging to H vibronic sub-bands ($K' = 5$). Although the calculations indicated that three or four lines should be present in the H vibronic sub-bands belonging to the strongest bands in the spectrum, it was not possible to make any unambiguous assignments of these lines owing to the scarcity of pairs of lines giving lower-state combination differences.

It was found that the bands of the principal progression $(0, v_2', 0) \leftarrow (0, 0, 0)$ accounted for the majority of the strong lines in the NH_2 absorption spectrum. Several strong lines remained unassigned, however, and it was noted that the $^{14}NH_2$–$^{15}NH_2$ isotope shifts of many of these lines were a few cm^{-1} smaller than the isotope shifts of other lines in the same spectral region. This suggested that the lines may belong to bands of a subsidiary progression $(1, v_2', 0) \leftarrow (0, 0, 0)$ involving the excitation of one quantum of the totally symmetric stretching vibration v_1'. This conclusion proved correct, and the lines were assigned without difficulty to four bands of the subsidiary progression. The rotational assignments for these bands are given in table 1. The lower-state combination differences agree with those obtained from the bands of the principal progression, confirming that the two progressions have a common lower state. A schematic diagram showing the bands of the principal and subsidiary progressions and the observed vibronic structures of these bands is given in figure 9.

The vibronic structures of the ND_2 bands were found to be very similar to those of the NH_2 bands. In addition to the Σ and Π sub-bands which have already been discussed, four Δ vibronic sub-bands and one Φ vibronic sub-band have been identified and the rotational assignments are given in table 2. The quadratic G factor for ND_2 is ~ 20 cm^{-1} compared with the value of 25 to 30 cm^{-1} for NH_2. One band of the subsidiary progression $(1, v_2', 0) \leftarrow (0, 0, 0)$ of ND_2 has also been identified, the rotational assignments being given in table 2. A schematic diagram showing the bands of the ND_2 spectrum which have been analyzed and the vibronic structures of these bands is given in figure 9.

Over 900 lines of the NH_2 absorption spectrum and 500 lines of the ND_2 absorption have been assigned, including more than 80% of the stronger lines in these spectra. Many of the unidentified lines undoubtedly belong to bands in the two progressions discussed above, but unambiguous assignments have not been possible owing to the lack of suitable combination differences. Some of the unidentified lines may belong to bands of other progressions or even to bands of a second electronic transition, although according to the arguments given in § 7 it is unlikely that the absorption spectrum should show a second allowed transition in the observed spectral region. Most of the stronger lines which have not been identified lie at the red end of the spectrum. It is possible that the

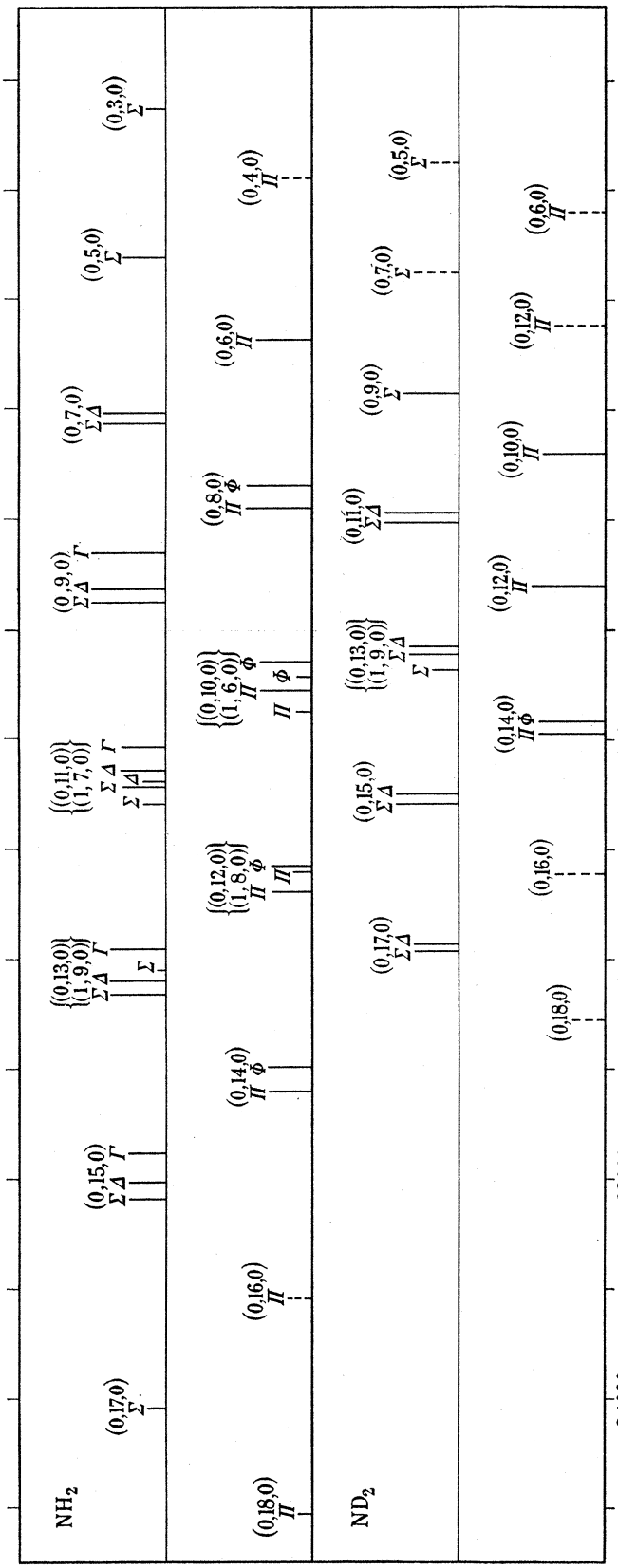

FIGURE 9. Schematic representation of the observed vibronic structures of the NH_2 and ND_2 spectra. Bands with odd and even v_2' have been plotted separately for the sake of clarity. Bands indicated by dashed vertical lines denote that clusters of absorption lines have been observed but no rotational analyses have been carried out.

difficulty encountered in making assignments in this region is due to the much larger spin splittings observed and to a change in the spin coupling. It is doubtful if any of the unidentified lines belong to bands originating in vibrationally excited levels in the ground state since the upper-state combination differences for such bands should be identical with differences found in the corresponding bands of the principal progression. No such agreement, however, has been found.

6. Evaluation of molecular constants

(a) *Rotational constants*

(i) *Ground state*

The ground-state rotational constants for NH_2 and ND_2 were obtained using the following combination relations:

$$\left.\begin{aligned} &{}^{R}R(2_{11}-1_{01})-{}^{P}Q(2_{11}-2_{21}) \\ &{}^{R}Q(1_{11}-1_{01})-{}^{P}P(1_{11}-2_{21}) \end{aligned}\right\} = (2_{21}-1_{01})'' = 4A^{*''}, \tag{7}$$

$$\left.\begin{aligned} &{}^{P}Q(1_{01}-1_{11})-{}^{P}P(1_{01}-2_{11}) \\ &{}^{R}R(2_{21}-1_{11})-{}^{R}Q(2_{21}-2_{11}) \end{aligned}\right\} = (2_{11}-1_{11})'' = 4B^{*''}, \tag{8}$$

$$\left.\begin{aligned} &{}^{P}R(2_{02}-1_{10})-{}^{P}Q(2_{02}-2_{12}) \\ &{}^{R}R(2_{20}-1_{10})-{}^{R}Q(2_{20}-2_{12}) \end{aligned}\right\} = (2_{12}-1_{10})'' = 4C^{*''}, \tag{9}$$

where $A^{*''}$, $B^{*''}$ and $C^{*''}$ denote the constants uncorrected for the effects of centrifugal distortion. The mean values for these combination differences averaged over all the bands are

	NH_2		ND_2	
$4A^{*''}$	94·50 cm^{-1}	(12)	53·25 cm^{-1}	(8)
$4B^{*''}$	51·76 cm^{-1}	(19)	25·93 cm^{-1}	(2)
$4C^{*''}$	32·66 cm^{-1}	(14)	17·19 cm^{-1}	(8)

where the numbers in brackets denote the number of individual determinations. The effects of spin doubling on these differences are small ($< 0{\cdot}3$ cm^{-1}) and have been removed by taking mean values for the spin components. Since the corrections for centrifugal distortion are small, and since the centrifugal distortion term values for NH_2 and ND_2 were found to be similar to the values for H_2O and D_2O (see below), the centrifugal distortion term values given by Benedict & Plyler (1951) for H_2O and by Benedict, Gailar & Plyler (1956) for D_2O were used to correct the above values of $A^{*''}$, $B^{*''}$ and $C^{*''}$. The values of the rotational constants of NH_2 and ND_2 corrected in this manner are given in table 5.

With these constants the ground-state rotational term values for NH_2 and ND_2 were calculated by the method of King *et al.* (1943) using the convenient tables of Turner, Hicks & Reitwiesner (1953). Tables of experimentally determined ground-state term values were constructed using the observed combination differences and assuming only the values for the $N = 1$ levels. For the latter, the calculated values were used and the centrifugal distortion corrections for H_2O and D_2O were adopted. The observed and calculated term values are given in tables 6 and 7 for NH_2 and ND_2, respectively, and the centrifugal-distortion correction terms are compared with the corresponding values

for H_2O and D_2O. It may be seen that there is a considerable similarity between the two sets of centrifugal-distortion term values, although the values for NH_2 and ND_2 are somewhat smaller than for H_2O and D_2O.

The values for the ground-state rotational constants were checked by the method described by Benedict & Plyler (1951) and Dalby & Nielsen (1956). By suitable averaging of the term values for all the levels of a given N the quantities A_N, B_N and C_N were obtained. These quantities were then plotted against $N(N+1)$ and the effective rotational constants A, B and C and the centrifugal distortion constants D_A, D_B and D_C obtained from the intercepts and slopes of the best straight lines (see figure 10). The effective rotational

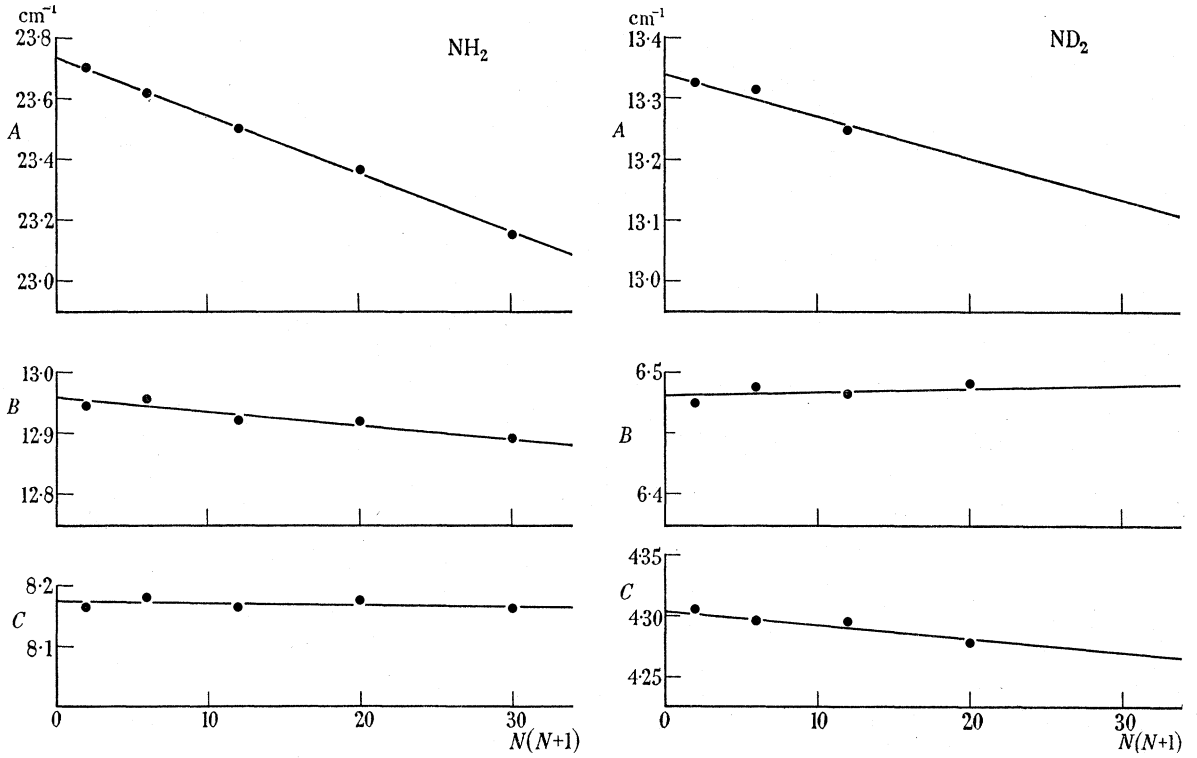

FIGURE 10. Graphical plots from which the rotational constants A, B and C and the centrifugal distortion constants D_A, D_B and D_C may be derived for the ground vibrational states of NH_2 and ND_2 (see text).

constants differ from the true constants by quantities of the order of magnitude of the centrifugal-distortion constants. Indeed the values obtained by the extrapolation procedure agree with those given in table 5 to within this accuracy (0·01 to 0·02 cm^{-1}). The values for the centrifugal distortion constants are given in table 5. The D_B and D_C distortion constants for NH_2 and ND_2 are very similar to those for H_2O and D_2O but the D_A constants are about 25% smaller.

The principal moments of inertia for NH_2 and ND_2 were calculated from the equation $I_X = (27{\cdot}9890\times10^{-40})/X$ ($X = A$, B or C) and are given in table 5. The inertial defects ($\Delta = I_C - I_A - I_B$) were also evaluated and agree closely with the defects determined by Benedict *et al.* (1956) for the vibrational ground states of H_2O ($\Delta = 0{\cdot}0807\times10^{-40}$ g cm^2) and D_2O ($\Delta = 0{\cdot}1075\times10^{-40}$ g cm^2). This agreement provides confirmatory evidence that the NH_2 and ND_2 bands originate in the vibrational ground states. Values for the

bond length and bond angle were calculated from I_A and I_B for both NH_2 and ND_2 (see table 5). The values agree well within the differences to be expected on account of zero-point vibration. If the I_C constants are used slightly different values are obtained, the differences being $\sim 0{\cdot}005$ Å in bond length and $\sim 30'$ in bond angle.

(ii) *Excited state*

Term values for the excited-state rotational levels were obtained by adding the appropriate ground-state term value to the wave number of each observed line. Since in general several values were obtained for each excited state level, mean values were taken and are given in tables 8 and 9 for NH_2 and ND_2 respectively.

For most of the Σ vibronic levels no spin splitting was detected, though for a few levels a small spin splitting was observed. In these levels the mean term value was used for the evaluation of rotational constants. For most of the bands, the term value of the $N = 0$ level and hence the origin of the Σ vibronic sub-band was obtained from the first line of the ${}^{P}P_{1,N-1}$ branch. These origins are accurate to a few hundredths of a cm^{-1} and are given in tables 10 and 11 for NH_2 and ND_2 respectively. For these bands the purely rotational parts of the term values were obtained by subtracting the term values of the $N = 0$ levels. These rotational term values were then expressed by the conventional formula

$$F'(N) = B'N(N+1) - D'N^2(N+1)^2, \tag{10}$$

and the constants B' and D' derived by plotting $F(N)/N(N+1)$ against $N(N+1)$. The values obtained are given in tables 12 and 13. For the few bands in which the term value of the $N = 0$ level could not be obtained directly from the spectrum, the origins and rotational constants were obtained in the manner described below for the Π vibronic sub-bands. It was found that while equation (10) gave a satisfactory representation of the rotational levels, the values of D' for the various bands are negative. This means that the coefficient D' can only be regarded as a coefficient in a power series expansion of the rotational energy, and cannot be interpreted as a centrifugal distortion constant.

For the Π vibronic levels, spin splittings up to 15 cm^{-1} and K-type splittings up to 40 cm^{-1} have been observed; both types of splitting show a marked variation with the rotational quantum number N and the vibrational quantum number v_2'. At low values of N the spin splitting is usually larger than the K-type splitting while the reverse is true at higher N values. The K-type splitting shows an approximate linear dependence on $N(N+1)$ similar to the splitting observed for the $K = 1$ levels of a slightly asymmetric top. Furthermore, the K-type splitting increases with increasing v_2' as might be expected since the average asymmetry of the molecule also increases. The spin splitting shows a marked dependence on the rotational quantum number N, and generally decreases with increasing N in a manner similar to that for a diatomic molecule in a ${}^2\Pi$ state with Hund's case (*a*) coupling. The spin splitting also decreases with increasing v_2' and even shows a reversal in sign at higher values of v_2'.

Attempts were made to fit the rotational term values to formulae similar to those which have been developed for diatomic molecules in ${}^2\Pi$ states with large Λ-doubling (Herzberg 1950, p. 232 *et seq.*). The data, however, did not extend for a sufficiently large range of N values to permit satisfactory tests of these formulae. Moreover, it has not been possible

to make unambiguous assignments of J values to the individual levels and hence to test whether the mean term values for levels with the same value of J obey the simple rotator formula as is found in the corresponding diatomic case. Since in general the effects of spin doubling and of K-type splitting are small compared with the separations between successive rotational levels, it was decided to take the mean of the term values for levels with equal N and to fit these mean values to the formula

$$T' = \nu_0^K + B'[N(N+1) - K^2], \tag{11}$$

neglecting higher terms. The constants ν_0^K and B' were obtained in the usual manner by plotting T' against $N(N+1)-K^2$. The origins of the Π vibronic sub-bands are given in tables 10 and 11 for NH_2 and ND_2 and are accurate to a few tenths of a cm^{-1}. The values for the rotational constant B' are given in tables 12 and 13 and are probably significant to 0·1 or 0·2 cm^{-1}.

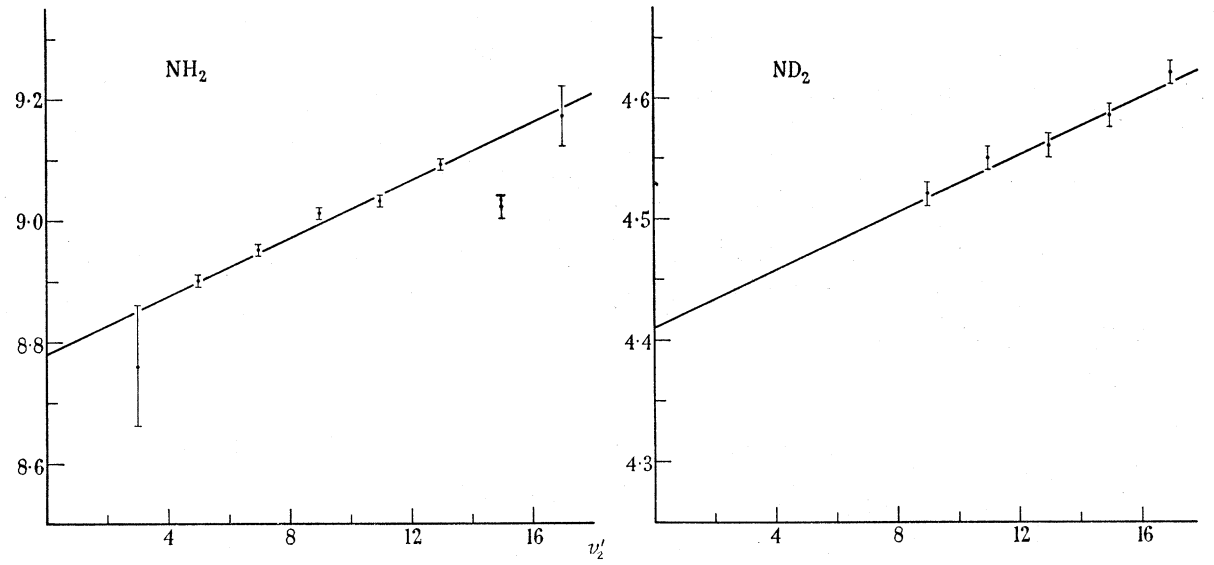

FIGURE 11. Variation of $B_{0v\,0}$ with v_2' for NH_2 and ND_2.

For the Δ, Φ and Γ vibronic levels the K-type splittings are very much smaller than those for the Π vibronic levels; for the Δ-vibronic levels the splittings are sometimes slightly negative. The spin splittings for the Δ, Φ and Γ vibronic levels are in general larger than the K-type splittings and increase with increasing K for comparable values of v_2' and N. In the absence of explicit formulae for the rotational levels, the sub-band origins and rotational constants were determined in the same manner as for the Π vibronic sub-bands. The values obtained for the various constants are given in tables 10 to 13.

The B' values for the Σ vibronic levels show a fairly smooth variation with the vibrational quantum number v_2'; for the other vibronic levels, however, the inaccuracies in the determination of the rotational constants mask any regularities in the variation of B' with v_2'. A marked increase in B' with increasing K' may, however, be noted. This latter variation is consistent with an increase in the bending of the molecule with increasing angular momentum about the axis. For the determination of B'_{000}, the B values for the Σ vibronic levels were plotted against v_2' (see figure 11) where the values of v_2' were determined in the manner described in §6(*b*). The data for NH_2 extend from $v_2' = 3$ to 17

and lie sufficiently close to a straight line to justify a linear extrapolation. For ND_2 the data are less extensive and no values have been obtained for $v_2' < 9$. By analogy with NH_2, however, a linear extrapolation was adopted. The values for B'_{000} and α'_2 are given in table 5. A value for α'_1 may also be obtained from the B values for the $(0, v_2', 0)$ and $(1, v_2', 0)$ levels. A tentative value is given in table 5, but it should be remembered that this value is probably not very reliable since the $(1, v_2', 0)$ levels are in resonance with $(0, v_2'-4, 0)$ levels (see §6(*c*)).

It is interesting to note that the values of α'_1 and α'_2 are respectively positive and negative in accordance with the behaviour expected for a linear triatomic molecule. Furthermore, the value of B'_{000} for NH_2 is equal to twice the corresponding value for ND_2 to within the experimental error, thus providing strong evidence for the linearity of the molecule in the upper state. On this basis the values of r'_{000} derived from the NH_2 and ND_2 data are 0·976 and 0·974 Å respectively, i.e. the bond length is about 0·05 Å shorter than in the lower state. It might be pointed out that in the absence of an exact theory to fit the observed rotational levels, the procedure adopted for the determination of B values is open to question. In particular the extrapolation of the B values for the Σ vibronic levels to obtain B'_{000} may not be valid; although the resultant angular momentum of the molecule about the axis is zero, there may still be equal and opposite amounts of nuclear and electronic angular momentum. The internal consistency of the results, however, justifies the belief that the above procedure is essentially correct and that the value for the bond length in the excited state is not in error by more than 0·01 Å. The significance of this short bond length will be discussed in §7.

(*b*) *Vibrational constants*

Before proceeding with the evaluation of vibrational constants for NH_2 and ND_2 we shall consider first the large vibronic splittings which have been observed in the upper state. It was found experimentally (see §5) that the splittings could be fitted approximately by a quadratic formula of type (6). The quadratic coefficients G for the various bands were determined from the splittings of the Σ–Δ and Π–Φ sub-bands and are given in tables 10 and 11 for NH_2 and ND_2. For a few of the NH_2 bands where the Γ sub-bands were observed, the values of G were obtained by taking the means of the values derived from the Σ–Δ, Σ–Γ and Δ–Γ splittings. Most of the G values were found to lie in the region of 28 cm^{-1} for NH_2 and 19 cm^{-1} for ND_2.

From equation (6) it is seen that there should be a staggering of the origins of the Π sub-bands relative to those of the Σ sub-bands by G cm^{-1} to lower frequencies. The effects of such a staggering can be clearly seen by plotting the vibrational intervals between successive bands of the principal progressions for NH_2 and ND_2 against the vibrational quantum number v_2'. A much larger scatter of the points is observed if the origins of the Π vibronic sub-bands are used rather than the values which have been corrected by the appropriate value of G. The corrected values are given in table 14 and were used for the evaluation of vibrational constants.

The vibrational numbering for bands of the principal progressions of NH_2 and ND_2 was obtained by extrapolating the observed progressions to lower frequencies until the differences between the calculated values for NH_2 and ND_2 could be explained on the basis of

the differences in the zero-point energies of the two molecules. It is known that the origin of the transition lies in the region of 9600 cm^{-1} from the $^{14}NH_2$–$^{15}NH_2$ isotope shifts; moreover, from the discussion given in §8 it is seen that bands with even K' values occur with odd values of v_2' and vice versa. With this information it is possible to determine the vibrational numbering given in table 14.

The vibrational constants $\omega_2^{0'}$ and $x_{22}^{0'}$ for NH_2 and ND_2 were determined by fitting the band origins to the quadratic formula

$$\nu_{0,v_2',0} = T'_{000}+\omega_2^{0'}v_2'+x_{22}^{0'}v_2'^2 \qquad (12)$$

by means of the method of least squares. The values obtained for the constants are given in table 5. It is seen that the values for the vibrational constants $\omega_2^{0'}$ are unusually low and are from 2 to 3 times smaller than the corresponding vibrational constants in other molecules, e.g. NH_3. Moreover, the anharmonic constants $x_{22}^{0'}$ are unusually large and have the opposite sign to those found for most linear triatomic molecules.

The calculated values for the band origins obtained using these constants are given in table 14. It may be noted that the deviations between some of the observed and calculated band origins are quite large. The large deviations and the reversal of sign in the regions of the (0, 12, 0) band for NH_2 and the (0, 14, 0) band for ND_2 are due to a strong Fermi-type interaction between (0, v_2', 0) and (1, $v_2'-4$, 0) levels. The effects of the interaction extend for several vibrational quanta and are discussed in more detail in §6(*c*). The large discrepancies for the lowest vibrational levels observed suggest that it would be interesting to extend the experimental data to still lower vibrational quantum numbers. The large deviations at the highest vibrational quantum numbers may be due to neglect of higher terms in the potential function. It is doubtful, however, if a significant improvement in the vibrational constants could be obtained by fitting a vibrational equation of higher order to the present data.

(*c*) *Fermi interaction constants*

The presence of a strong Fermi-type interaction between vibrational levels of the type (0, v_2', 0) and (1, $v_2'-4$, 0) was inferred from (i) the behaviour of the differences between the observed and calculated band origins for the (0, v_2', 0) levels (see table 14), and (ii) the discontinuity in the value of $\nu_0(0, v_2', 0)-\nu_0(1, v_2'-4, 0)$ between $v_2' = 12$ and 13 for NH_2 (see table 15). It was noted, moreover, that bands of the subsidiary progression (1, v_2', 0) ← (0, 0, 0) were observed only in regions of close resonance, the intensity being greater the closer the resonance. In the absence of any observed sub-levels which are not affected by the resonance, it was not possible to derive an accurate value for the matrix element W_{ni} of the perturbation function. A value was obtained, however, by plotting the absolute magnitude of the difference $\nu_0(1, v_2'-4, 0)-\nu_0(0, v_2', 0)$ against v_2' and drawing a smooth curve through the points. From the value of the difference at the minimum of the curve it was deduced that $W_{ni} = 72\pm3$ cm^{-1}, depending on the particular curve drawn. It should be pointed out that this method neglects the variation of W_{ni} with vibrational quantum number v_2'. Since only one band in the subsidiary progression was observed for ND_2 it was only possible to obtain an upper limit for the value of W_{ni}, namely $W_{ni} \leqslant 68{\cdot}3$ cm^{-1}. It is interesting to note that Robinson & McCarty (1959 have

independently obtained a value for $W_{ni} \sim 75$ cm^{-1} for NH_2 by measuring the relative intensities of the resonating pairs in the solid state at low temperatures and assuming that the subsidiary progression obtains all its intensity by resonance. The agreement between the two independent values confirms that this mechanism is substantially correct.

It may be noted that this is the first example of a vibrational resonance between two levels differing by 4 units in one of the vibrational quantum numbers. The perturbation function W_{ni} in such a case will depend on fifth-order potential constants. The magnitudes of the shifts of the various levels due to the resonance were calculated by standard procedures (Herzberg 1945, p. 216) and are given in table 15. The quantities a^2 and b^2, which are proportional to the relative intensities of the resonating components, were also calculated.

From the corrected values for the origins of bands of the subsidiary progression the vibrational constants $\omega_1^{0\prime}+x_{11}^{0\prime}$ and $x_{12}^{0\prime}$ were derived using the relation

$$\nu_0(1, v_2', 0)-\nu_0(0, v_2', 0) = \omega_1^{0\prime}+x_{11}^{0\prime}+v_2'x_{12}^{0\prime}. \qquad (13)$$

For $v_2' = 6$, 7, 8 and 9 the values of these differences are, respectively, 3356·2, 3413·8, 3364·8 and 3373·2 cm^{-1}. The value for $v_2' = 7$ is not consistent with the other values, and may be due to a further unexplained resonance. From the other values it was deduced that $\omega_1^{0\prime}+x_{11}^{0\prime} \sim 3325$ cm^{-1} and $x_{12}^{0\prime} \sim 5$ cm^{-1} (see table 5). For ND_2 the only additional information which could be derived from the single band observed in the subsidiary progression is $\omega_1^{0\prime}+x_{11}^{0\prime}+9x_{12}^{0\prime} \sim 2517$ cm^{-1}, neglecting the effects of the Fermi resonance.

7. Nature of the electronic transition

According to the orbital considerations of Walsh (1953), the electron configuration and term-type of the ground state of NH_2 is expected to be

$$K(a_1)^2\,(b_2)^2\,(a_1)^2\,(b_1), \quad {}^2B_1,$$

and of the low-lying excited states:

$$K(a_1)^2\,(b_2)^2\,(a_1)\,(b_1)^2, \quad {}^2A_1,$$
$$K(a_1)^2\,(b_2)\,(a_1)^2\,(b_1)^2, \quad {}^2B_2.$$

The observed transition should correspond to the allowed transition ${}^2A_1 \leftarrow {}^2B_1$ rather than to the forbidden transition ${}^2B_2 \leftarrow {}^2B_1$. These conclusions are in agreement with the earlier predictions of Mulliken (1943).

The ground state may be shown to be a B state rather than an A state from the alternation which has been observed in the intensities of successive lines in the different branches of the NH_2 and ND_2 spectra (see figures 1 to 4). For NH_2 the lines originating in the 0_{00} level of the ground state are strong, whereas for ND_2 the corresponding lines are weak. Since H nuclei obey Fermi statistics the total eigenfunction must be of species B (Herzberg 1945, p. 465). For the 0_{00} level of NH_2 the nuclear spin function and the rotational eigenfunction are both of species A. Since the vibrational eigenfunction is totally symmetric, the electronic eigenfunction must therefore be of species B. The same

conclusion concerning the electronic symmetry may be deduced from the ND_2 data. The intensity alternation therefore shows that the ground state is either a B_1 or a B_2 state. The observed bands however obey type C selection rules and can only be assigned to an $A_1 \longleftrightarrow B_1$ or an $A_2 \longleftrightarrow B_2$ transition. Since a low-lying A_2 state is not possible from simple valence arguments, the intensity alternation and selection rules lead to the conclusion that the ground state is a B_1 state and the excited state an A_1 state. The observed spin splittings are consistent with a doublet character for both states.

Walsh (1953) predicted that the transition should be accompanied by an increase of the apex angle in the equilibrium form of the upper state. Moreover, since the electron configuration of the ground state differs from that of H_2O only by the removal of one non-bonding electron in a b_1 orbital with a node in the plane of the molecule, the bond angles in both molecules should be very similar. Both predictions are in accordance with the results of our analysis. In 1958 Walsh expressed the view that NH_2 may not be linear in its excited state, but may have a small potential maximum in the 180° configuration. He cited the large negative anharmonicity† of the bending vibration in support of this idea. The vibronic structure, however, shows clearly that NH_2 behaves as a linear molecule above the (0, 3, 0) level, which is the lowest level so far observed, although it does not preclude the existence of a very small potential maximum in the 180° configuration. The rotational analysis shows that the B'_{000} value for NH_2 is equal to twice the value for ND_2 to within experimental error (see §6(*a*)). If a linear equilibrium configuration is assumed a reasonable value for the NH bond length is obtained.

As regards the NH bond length, Walsh (1953) predicted that there should be little change of bond length accompanying the transition since the outermost (a_1) and (b_1) orbitals are essentially non-bonding. The experimental value for the bond length in the excited state is, however, 0·05 Å shorter than in the ground state and we believe this shortening to be significant. According to the orbital diagram given by Walsh (1953), the $^2A_1$ and $^2B_1$ states both correlate with a $^2\Pi_u$ state in the linear configuration having the electronic structure $K(\sigma_g)^2\,(\sigma_u)^2\,(\pi_u)^3$, where the π molecular orbitals approximate to $2p\pi$ atomic orbitals of the nitrogen atom. When the molecule bends, two configurations are possible, namely $K(\sigma_g)^2\,(\sigma_u)^2\,(\pi_z)^2\,(\pi_x)$ and $K(\sigma_g)^2\,(\sigma_u)^2\,(\pi_z)\,(\pi_x)^2$, depending on whether the odd electron is in a π orbital perpendicular to the plane of bending (π_x) or parallel to the plane of bending (π_z). The latter configuration corresponds to the excited state of NH_2; it may be noted that the (σ_g) and (σ_u) orbitals are sp hybrid valencies linking the hydrogen atoms to the central nitrogen atom. The former configuration is apparently unstable in the linear configuration and rearranges to the configuration $K(a_1)^2\,(b_2)^2\,(a_1)^2\,(b_1)$, where the inner a_1 and b_2 orbitals are predominantly p-type valencies linking the hydrogen atoms to the nitrogen atom (the valencies would be pure p-type if the bond angle were 90°). The outer a_1 orbital is essentially a non-bonding s orbital and the b_1 orbital a non-bonding $2p\pi$ orbital on the nitrogen atom. The N—H bonding thus changes from predominantly a p-type valency in the ground state with a small admixture of s character, to a sp hybrid valency in the excited state. The decrease in bond length is similar to the corresponding decrease which has been observed for C—H bonds (Walsh 1947).

† We have chosen to identify negative anharmonicity with the less common behaviour in triatomic molecules, i.e. positive values of x_{22}. There is no accepted usage of this term.

From simple hybridization considerations we might expect a regular variation of N—H bond length with H—N—X bond angle in a series of compounds. The following data bear out this expectation:

	$NH_2(^2A_1\Pi_u)$	HNCO (*a*)	NH_3 (*b*)	$NH_2(^2B_1)$	NH (*c*)
r_0(NH) (Å)	0·975	1·000	1·017	1·024	1·048
∠ H—N—X	180°	125·5°	107·8°	103·3°	(90°)

(*a*) Reid (1950), (*b*) Benedict & Plyler (1957), (*c*) Herzberg (1950).

where it is assumed that the bonding in the NH radical is pure p-bonding corresponding to a nominal bond angle of 90°. The NH bond lengths for both states of NH_2 are thus consistent with values obtained from other compounds.

8. Discussion of the Renner effect

The complex vibronic structures observed in the excited states of NH_2 and ND_2 may be understood in terms of an interaction between electronic and vibrational motions, first discussed in detail by Renner (1934) for linear molecules. For states with $\Lambda \neq 0$ the electronic angular momentum $\Lambda h/2\pi$ about the internuclear axis couples with the angular momentum $lh/2\pi$ associated with the bending vibration to form a resultant $Kh/2\pi$, where $K = |l \pm \Lambda|$. K is a good quantum number for any degree of interaction, but l and Λ may no longer be significant quantum numbers. For a given value of v, the quantum number representing the bending vibration, the possible values of K are $v+\Lambda$, $v+\Lambda-2$, $v+\Lambda-4$, ..., 1 or 0, depending on whether $v+\Lambda$ is odd or even. For $\Lambda = 1$, all values of K occur twice except for the value $K = v+1$.

The energy separations between the various levels with a given value of v but different values of K can be calculated if the potential energy functions governing the bending of the molecule are known. Two such potential energy functions in general arise from the splitting of degeneracy of the linear molecule by the bending vibration. Renner let $V^+(r)$ and $V^-(r)$ represent the electronic energies for fixed nuclei of the two states with higher and lower energy respectively, where r denotes the deviation of the framework from linearity. The eigenfunction of one of these states is symmetric, and the other antisymmetric with respect to the plane given by the three nuclei, the order of the energies depending on the electronic structures of the two states.

Three general cases of the Renner effect are possible, corresponding to the three types of potential curve shown in figure 12. In the first case both curves have a minimum in the 180° configuration (figure 12*a*); this is the case discussed by Renner (1934). The second possibility is that the upper curve has a minimum and the lower curve a maximum in the 180° configuration (figure 12*b*); this is the case found for NH_2. The third possibility is that both curves show a maximum in the 180° configuration (figure 12*c*).

Renner carried out detailed calculations on the vibronic structures to be expected for electronic Π states corresponding to case (*a*). He showed that while the energies of the Σ vibronic levels were determined by the upper and lower potential curves individually, the energies of the other vibronic levels ($K > 0$) were dependent on the forms of both potential

curves. He obtained an equation for the energies of the vibronic levels with $K > 0$ by means of a second-order perturbation calculation involving terms in r^2 and expressed the results in terms of a parameter ϵ, where $\epsilon = (V^+ - V^-)/(V^+ + V^-)$. The results were considered to be valid for $0 < \epsilon < 0{\cdot}4$. Renner also carried out a more elaborate infinite matrix calculation on the energies of the Π vibronic levels over the complete range of ϵ from 0 to 1. A diagram showing the vibronic structure to be expected for the first few vibrational levels ($v_2 = 0$ to 5) of an electronic Π state with $\epsilon = 0{\cdot}15$ is shown in figure 13 (b). For comparison purposes the corresponding structure for an electronic Σ state is shown in figure 13 (a). Our representation of the levels for the Π state is slightly different from that of Renner in that we choose to keep V^+, and hence the energies of the upper Σ levels, constant, whereas Renner keeps the sum $V^+ + V^-$ constant. The conversion is readily achieved by dividing the energies obtained from Renner's formulae by $\sqrt{(1+\epsilon)}$.

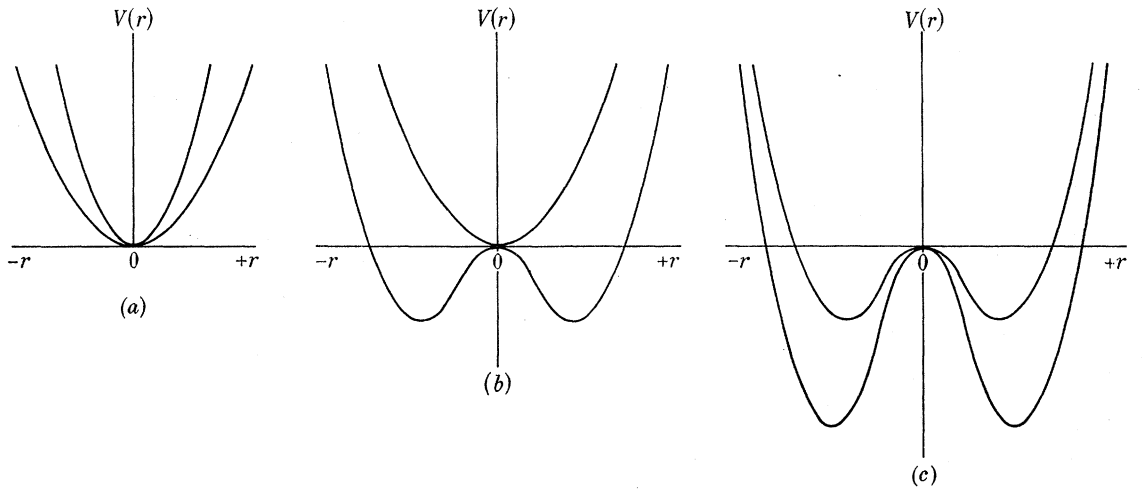

FIGURE 12. Three types of potential curves for states derived by the splitting of doubly degenerate electronic states.

In the case of NH_2 (and ND_2) the observed vibronic splittings are much larger than those which would be predicted by Renner's formulae for values of $\epsilon < 1$. Moreover, for each value of v_2' only one sub-level is observed for each value of K, the levels appearing in the order Σ, Δ, Γ, ... and Π, Φ, ... with *decreasing* energy. These observations may be qualitatively explained if it is remembered that the ground state and the excited state both correlate with a common $^2\Pi_u$ state (see §7 and figure 12b), i.e. that $\epsilon > 1$ for NH_2. Each state may in effect be regarded as 'half a Π state'; since the upper state has a linear equilibrium configuration we choose to denote it by the symbol $^2A_1\Pi_u$. The detailed correlation between the vibronic levels of a Π_u state and the corresponding levels of an $A_1\Pi_u$ and a B_1 state may be inferred by considering the behaviour of the vibronic levels as $\epsilon \to 1$. Renner showed that while the energies of the Σ vibronic levels associated with the upper potential curve remained finite even for $\epsilon > 1$, the energies of the Σ vibronic levels associated with the lower potential curve approach zero as $\epsilon \to 1$ and have no real values for $\epsilon > 1$. We may assume, therefore, that in the latter case the levels are no longer stable in a linear configuration but must be correlated with the appropriate levels of a bent molecule. In the process of bending the total angular momentum of the molecule

about the axis for the linear molecule correlates with the rotational angular momentum of the molecule about the figure axis for a slightly bent molecule. The detailed correlation for the Σ vibronic levels is shown in figure 13*c*. We have assumed for simplicity that the lower state approximates to a symmetric top and we have correlated the unstable Σ vibronic levels with the lowest available $K = 0$ rotational levels associated with the various quanta of the bending vibration.

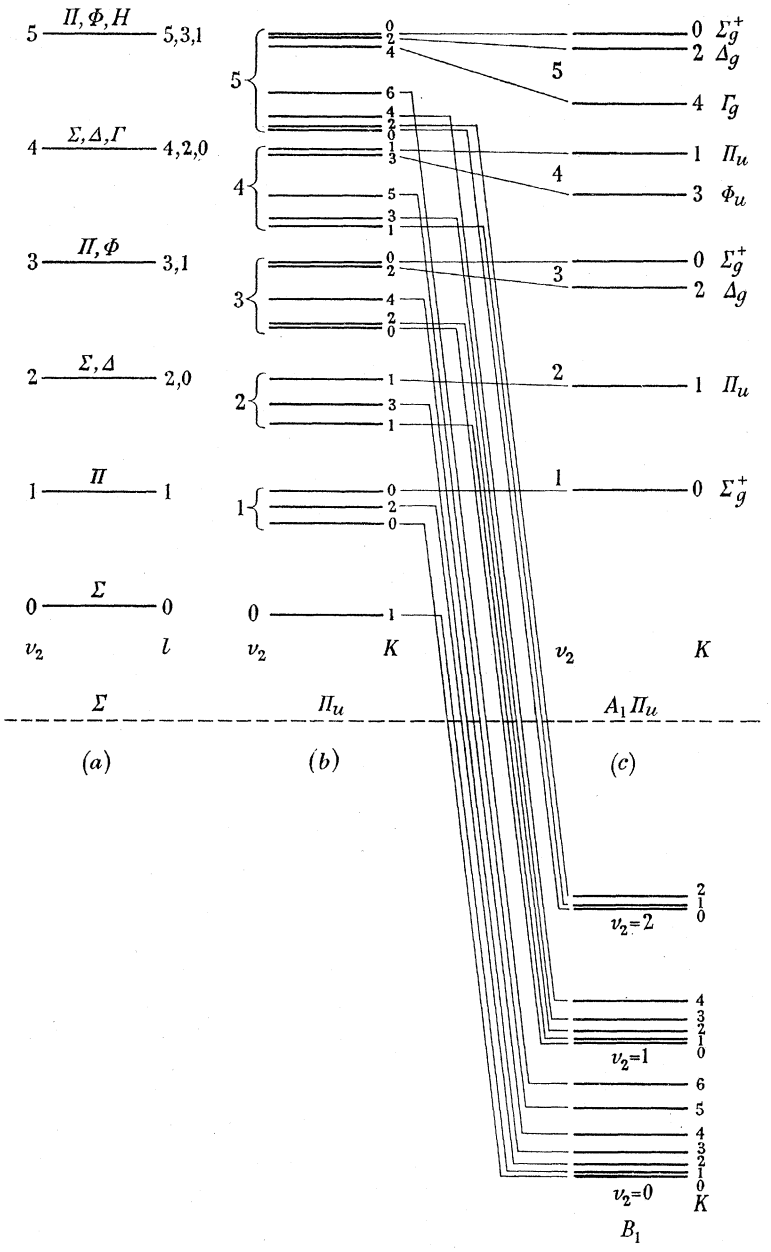

FIGURE 13. Schematic diagram of the first few energy levels and vibronic species for the bending vibration of a linear triatomic molecule (*a*) for an electronic Σ state, (*b*) for an electronic Π_u state with $\epsilon = 0{\cdot}15$. On the right-hand side of the diagram the correlation is given between the vibronic levels of the Π_u state and the corresponding levels of a bent B_1 and a linear $A_1\Pi_u$ state, neglecting the effects of the non-crossing rule. The vibronic splittings in (*c*) have been reduced to one-third of the splittings predicted for NH_2 by the theory of Pople & Longuet-Higgins, to avoid overlap of neighbouring levels.

For the Π vibronic levels Renner carried out a detailed calculation which showed that for $v_2 = 2, 4, 6, \ldots$, the energies of the upper Π vibronic levels remain finite while the energies of the lower Π vibronic levels approach zero as $\epsilon \to 1$. Furthermore, the energy of the single Π vibronic level with $v_2 = 0$ also approaches zero as $\epsilon \to 1$. We have assumed, therefore, that for $\epsilon > 1$ the upper Π vibronic levels correlate with stable Π levels in the $A_1\Pi_u$ state, while the lower Π vibronic levels (including the one with $v_2 = 0$) correlate with the $K = 1$ rotational levels associated with successive quanta of the bending vibration in the B_1 state (see figure 13*c*). It should be pointed out that while our correlation, strictly speaking, violates the non-crossing rule (see Renner 1934, fig. 2, p. 190), the net result is the same as if the non-crossing rule were observed. The correlations for the higher vibronic levels are carried out in a similar manner to those for the Σ and Π vibronic levels. In each group of vibronic levels for the Π_u state, characterized by the same value for the vibrational quantum number, the uppermost levels with $K \leqslant v_2 - 1$ correlate with vibronic levels of the $A_1\Pi_u$ state while the other vibronic levels correlate with vibrational and rotational levels of the B_1 state.

Pople & Longuet-Higgins (1958) have carried out a quantitative treatment of the vibronic structure of the excited state of NH_2. They represented the potential curves for the upper and lower states by the equations

$$V^+ = \tfrac{1}{2}r^2 + hr^4, \tag{14}$$

$$V^- = (\tfrac{1}{2} - f)\, r^2 + gr^4, \tag{15}$$

where $f > \frac{1}{2}$, $g > 0$ and the unit of energy is the energy associated with the classical vibration frequency in the upper state. Using a first-order perturbation calculation they showed that the approximate energies of the upper-state vibronic levels are given by

$$E^+(n, K) = n - \tfrac{1}{2}f[n - \sqrt{(n^2 - K^2)}] + \tfrac{1}{4}(g+h)\,(3n^2 - K^2) - \tfrac{3}{4}(g-h)\, n\sqrt{(n^2-K^2)}, \tag{16}$$

where $n = v_2 + 1$. For values of $K \ll n$ an expansion to order K^2 gives

$$E^+(n, K) = n + \tfrac{3}{2}hn^2 - \tfrac{1}{8}K^2[2fn^{-1} - g + 5h]. \tag{17}$$

For the Σ vibronic levels ($K = 0$) the energy reduces to

$$E^+(n, 0) = n + \tfrac{3}{2}hn^2. \tag{18}$$

By fitting the observed energies of the Σ levels to this equation, values of h were obtained for NH_2 and ND_2 (see below).

If the coefficient in square brackets in equation (17) is positive, the theory predicts a quadratic lowering of levels with $K > 0$ in agreement with experiment. Values for f and g may be determined from the valency angle in the ground state and from the height of the barrier, in the manner described by Pople & Longuet-Higgins. The barrier height will be close to the values of T_{000} determined from the origins of the vibrational progressions for NH_2 and ND_2 (see § 6 (*b*)). Owing to the uncertainty of the corrections to be applied for the effects of zero-point vibration, a value of 10000 cm^{-1} for the barrier height was adopted. The values obtained for the coefficients f, g and h are:

	f	g	h
NH_2	$2{\cdot}7_{70}$	$0{\cdot}076_{95}$	$0{\cdot}012_{84}$
ND_2	$3{\cdot}2_{89}$	$0{\cdot}078_{90}$	$0{\cdot}013_{37}$

When these are substituted into equation (16), values for $E^+(n, K)$ are obtained from which the wave numbers of the various vibronic levels are readily obtained. The calculated frequencies are given, to the nearest 10 cm^{-1}, in tables 10 and 11 for NH_2 and ND_2 together with the experimentally observed values.

The general agreement between the observed and calculated frequencies provides strong support for the interpretation of the spectrum given above. The close agreement for the Σ levels is, of course, to be expected since the value of h was determined from the best fit of these levels. For the other vibronic levels the agreement is closest for $K = 1$ and worst for $K = 4$. Reasons for the increasing discrepancies with increasing K value have been discussed by Pople & Longuet-Higgins.

By comparing equations (17) and (6) we see that, provided $g-5h \ll 2fn^{-1}$ as is the case for NH_2 and ND_2, the quadratic G factor should bear an inverse relationship to the vibrational quantum number. The experimental data in tables 10 and 11, however, are not in agreement with this prediction. Some of the experimental values are undoubtedly influenced by the vibrational perturbation discussed in § 6 (*c*), but on the whole the values do not show any systematic variation with the vibrational quantum number.

Two further points may be noted. First, the vibronic levels in the $^2A_1\Pi_u$ state (see figure 13*c*) are formally similar to those for an electronic Σ state with a large anharmonicity of the bending vibration. A criterion is needed therefore to determine whether or not a Renner effect is present. In the absence of any coupling between electronic motion and the bending vibration the two potential surfaces V^+ and V^- coincide, i.e. $f = 0$ and $g = h$. Under these circumstances equation (17) reduces to

$$E^+(n, K) = n+\tfrac{1}{2}h(3n^2-K^2). \tag{19}$$

Thus a Renner effect is indicated only if the K dependence of the energy levels is greater than that predicted by equation (19), as indeed is found in the case of NH_2.

Secondly, the energy of the lowest stable vibronic level of the $A_1\Pi_u$ state is of particular interest. In the correlation process shown in figure 13*b* and *c*, the lowest vibronic level of the Π_u state with $v_2 = 0$ correlates with the $K = 0$, $v_2 = 0$ level of the bent molecule. The lowest stable level in the $A_1\Pi_u$ state is derived from a vibronic level with $v_2 = 1$ in the Π_u state. In general, vibronic levels of the $A_1\Pi_u$ state with even value of K may be assigned odd vibrational quantum numbers and vice versa. From equation (18) we see that the energy of the lowest level is $E^+(2, 0) = 2$, neglecting anharmonicity. By contrast the contribution of the bending vibration to the energy of the lowest vibrational level of a linear molecule in a Σ electronic state is only one quantum of the bending vibration. An $A_1\Pi_u$ state thus represents a hitherto unobserved kind of state with a contribution of two quanta of the bending vibration to the energy of the lowest level. It would be very interesting to verify this prediction experimentally. With longer path lengths it should be possible to observe the lowest level for NH_2 and to determine from a study of vibrational isotope shifts the contribution of the bending vibration to the zero-point energy.

9. General discussion and conclusion

Although the principal features of the NH_2 and ND_2 absorption spectra have been satisfactorily assigned, many of the finer details of the spectra remain unexplained. Numerous weak lines and some of the stronger lines, especially those at the red end of the spectrum, have not been assigned; difficulty has been encountered in making unambiguous assignments in the regions of the (0, 4, 0) and (0, 16, 0) bands. The problem of rotational assignments however is an endless one, since almost any number of rotational lines could probably be observed, especially in emission.

The analysis has afforded many features of interest, some of which merit further investigation. The general question of rotational line intensities is worthy of further study both from a theoretical and an experimental viewpoint, the more so since the NH_2 molecule is of considerable importance in astrophysical problems. The table of line strengths for asymmetric rotors given by Cross *et al.* (1944) applies strictly to the case where the asymmetry of the lower state is the same as for the upper state. This is far from true in the case of NH_2. Nevertheless, we have found the results of Cross *et al.* very useful in gaining a semi-quantitative understanding of the intensities of the rotational transitions for NH_2. From the observed rotational intensity distributions within various branches we have been able to infer that the rotational temperature of the NH_2 radicals approximates to room temperature. In tables 1 and 2 we give two sets of values for the calculated rotational intensities of NH_2 and ND_2 assuming that (i) both states have the same asymmetry as the upper state, and (ii) both states have the same asymmetry as the lower state. In branches for which the two sets of values agree closely, the calculated values are in good agreement with the experimentally observed relative intensities. In cases where the two sets of calculated values diverge considerably, the observed intensities generally lie closer to the results of the first calculation. More exact values for the line strengths could be calculated in the manner discussed by Allen (1954); experimentally, the rotational line intensities could be conveniently studied in emission by means of photo-electric recording.

The ground state appears to behave in the normal manner for an asymmetric top, at least in the (0, 0, 0) vibrational level which is the only level which has so far been observed. A small spin splitting of the levels due to the coupling of electron spin with the rotational motion of the molecule has been observed. No quantitative explanation of the splittings has been given but qualitatively it may be stated that the splitting increases as expected with increasing J and also with increasing value of K_a. Information concerning the higher vibrational levels should be obtainable from the emission spectrum, especially as combination differences for the excited-state vibrational levels are now known. Such information would be especially interesting for levels near the top of the barrier since departures from normal behaviour are then to be expected.

The excited state shows several unusual features. The complex vibronic structure has been explained qualitatively in terms of the Renner effect by ourselves and quantitatively by Pople & Longuet-Higgins. It would be interesting to extend the observations to higher K values and also to lower v_2 values. No satisfactory formula has been obtained to fit the observed rotational term values for the Π, Δ, Φ and Γ levels and to account for the observed spin splitting and K-type doubling. The Σ rotational levels fit closely to the usual rotational formula for a linear molecule though only with a negative value for D. The

excited state might be expected to be an inverted doublet since it is derived from a $^2\Pi_u$ state which, from electron configuration arguments, should also be inverted. Unfortunately it has not been possible to assign J values unambiguously to test this prediction. The reversal in the sign of the spin splitting at the higher vibrational quantum numbers remains unexplained.

Several perturbations have been observed in the excited state. A new kind of Fermi interaction between vibrational levels of the type $(0, v_2, 0)$ and $(1, v_2-4, 0)$ has been found and a value of W_{ni} determined. It would be interesting to calculate the dependence of this quantity on the higher-order potential constants. In addition, several rotational perturbations have been observed: the effects of these perturbations in general extend for only a few J values and often affect only one component of a spin doublet. Examples of rotational perturbations may be seen in figures 1*a* and 2*c*.

In spite of the many unsolved problems a considerable understanding of the complex NH_2 spectrum has now been achieved. From the detailed rotational and vibrational analyses, the observed intensity alternations and the isotope shifts with nitrogen-15 and deuterium, there can no longer be any doubt that the carrier of the α-bands of ammonia is the free NH_2 radical.

We are indebted to Professor H. C. Longuet-Higgins, F.R.S., and Dr J. A. Pople for valuable discussions concerning the Renner effect and for communicating their manuscript to us in advance of publication. We wish to thank Miss L. L. Howe for assistance with the calculations.

References

Allen, H. C. 1954 *J. Chem. Phys.* **22**, 83.
Benedict, W. S., Gailar, N. & Plyler, E. K. 1956 *J. Chem. Phys.* **24**, 1139.
Benedict, W. S. & Plyler, E. K. 1951 *J. Res. Nat. Bur. Stand.* **46**, 246.
Benedict, W. S. & Plyler, E. K. 1957 *Canad. J. Phys.* **35**, 1235.
Bernstein, H. J. & Herzberg, G. 1948 *J. Chem. Phys.* **16**, 30.
Callomon, J. H. & Ramsay, D. A. 1957 *Canad. J. Phys.* **35**, 129.
Cross, P. C., Hainer, R. M. & King, G. W. 1944 *J. Chem. Phys.* **12**, 210.
Dalby, F. W. & Nielsen, H. H. 1956 *J. Chem. Phys.* **25**, 934.
Dennison, D. M. 1931 *Rev. Mod. Phys.* **3**, 280.
Dressler, K. & Ramsay, D. A. 1957 *J. Chem. Phys.* **27**, 971.
Edlén, B. 1953 *J. Opt. Soc. Amer.* **43**, 339.
Harrison, G. R. 1939 *M.I.T. Wavelength Tables.* New York: John Wiley and Sons, Inc.
Herzberg, G. 1945 *Infrared and Raman spectra of polyatomic molecules.* New York: D. Van Nostrand, Inc.
Herzberg, G. 1950 *Spectra of diatomic molecules.* New York: D. Van Nostrand, Inc.
Herzberg, G. & Ramsay, D. A. 1952 *J. Chem. Phys.* **20**, 347.
Herzberg, G. & Ramsay, D. A. 1953 *Disc. Faraday Soc.* **14**, 11.
Herzberg, G. & Teller, E. 1933 *Z. Phys. Chem.* B, **21**, 410.
King, G. W., Hainer, R. M. & Cross, P. C. 1943 *J. Chem. Phys.* **11**, 27.
Mulliken, R. S. 1943 Quoted in Swings, P., McKellar, A. & Minkowski, R. *Astrophys. J.* **98**, 142.
Pople, J. A. & Longuet-Higgins, H. C. 1958 *Mol. Phys.* **1**, 372.
Ramsay, D. A. 1953 *J. Phys. Chem.* **57**, 415.
Ramsay, D. A. 1956 *J. Chem. Phys.* **25**, 188.
Ramsay, D. A. 1957*a* *Ann. N.Y. Acad. Sci.* **67**, 485.
Ramsay, D. A. 1957*b* *Mém. Soc. Roy. Sci. Liège*, **18**, 471.

Reid, C. 1950 *J. Chem. Phys.* **18**, 1544.
Renner, R. 1934 *Z. Phys.* **92**, 172.
Robinson, G. W. & McCarty, M., Jr. 1959 *J. Chem. Phys.* **30**, 999.
Turner, T. E., Hicks, B. L. & Reitwiesner, G. 1953 *Asymmetric rotor eigenvalue table*, Ballistic Research Laboratories Report No. 878, Aberdeen Proving Ground, Maryland, U.S.A.
Walsh, A. D. 1947 *Disc. Faraday Soc.* **2**, 18.
Walsh, A. D. 1953 *J. Chem. Soc. Lond.* p. 2260.
Walsh, A. D. 1958 Quoted in Laidler, K. J. & Ramsay, D. A. *Canad. J. Chem.* **36**, 1.
White, J. U. 1942 *J. Opt. Soc. Amer.* **32**, 285.

TABLE 1. VACUUM WAVE NUMBERS, VIBRATIONAL AND ROTATIONAL ASSIGNMENTS FOR LINES OF THE NH_2 ABSORPTION SPECTRUM

(A) Bands involving Σ, Δ, Γ vibronic levels in the upper state

I. Σ vibronic levels

branch		rotational transition	calculated relative intensity		(0, 3, 0) band	(0, 5, 0) band	(0, 7, 0) band	(0, 9, 0) band	(0, 11, 0) band	(0, 13, 0) band	(0, 15, 0) band	(0, 17, 0) band	(1, 7, 0) band	(1, 9, 0) band
C.H.K. notation	our notation		$\kappa=-1$	$\kappa=-0{\cdot}386$										
${}^{ce}R_{\bar{1},2}$	${}^{P}R_{1,N-1}$	2_{02}–1_{10}	1·40	0·75	—	13 635·80	15 137·41 37·09	16 759·29 59·01	18 447·88	20 329·77	22 193·91	—	—	—
		3_{03}–2_{11}	6·70	2·32	—	13 642·55	15 144·48 44·16	16 766·75 66·53	18 455·25	20 338·09	22 202·93	24 118·96	18 606·66	—
		4_{04}–3_{12}	2·40	0·52	—	13 645·86	15 146·96	16 770·33 69·95	18 459·28	20 344·35	22 209·82	—	18 608·70	—
		5_{05}–4_{13}	6·22	0·86	—	13 638·38	15 147·35	16 771·16 69·20	18 461·74	20 345·19	22 218·09*	—	18 607·90	—
		6_{06}–5_{14}	1·53	0·15	—	—	15 147·84	16 772·62 72·19	18 464·72	20 350·20	22 230·94	—	18 607·24	—
		7_{07}–6_{15}	3·02	0·23	—	—	15 152·84 52·25	16 777·10	18 470·61	20 359·96	—	—	—	—
${}^{co}Q_{\bar{1},0}$	${}^{P}Q_{1,N}$	1_{01}–1_{11}	12·87	12·87	12 266·94	13 604·83	15 106·25 06·03	16 727·84 27·57	18 416·33	20 298·00	22 162·61	24 074·41	18 569·93	20 074·49
		2_{02}–2_{12}	5·98	6·90	12 263·86	13 603·05	15 104·67 04·52	16 726·50	18 414·90*	20 296·96*	22 161·12	—	18 567·40	—
		3_{03}–3_{13}	19·24	25·47	12 261·24	13 601·37*	15 103·28 03·07	16 725·70* 25·49*	18 414·10	20 296·96*	22 161·79	24 077·83	18 565·51	20 070·89
		4_{04}–4_{14}	5·18	8·50	—	13 601·37*	15 102·51	16 725·70* 25·49*	18 414·90*	20 299·78	22 165·28	—	18 564·15*	—
		5_{05}–5_{15}	13·87	21·67	12 257·04	13 594·76	15 103·73	16 727·57 25·49*	18 418·02	20 301·42	22 174·32	—	18 564·15*	—
		6_{06}–6_{16}	3·28	5·35	—	—	15 107·30	16 732·05 31·48	18 424·05	20 309·36	22 190·08	—	18 566·26	—
		7_{07}–7_{17}	6·31	10·62	—	—	15 115·73 14·98	16 739·90	18 433·41	20 322·75	22 218·09*	—	—	—
${}^{ce}P_{\bar{1},0}$	${}^{P}P_{1,N-1}$	0_{00}–1_{10}	2·80	2·80	—	13 582·24	15 083·54	16 705·05	18 393·58	20 275·04	22 139·26	—	18 547·28	—
		1_{01}–2_{11}	10·04	10·04	12 215·13	13 553·06	15 054·48 54·30	16 676·09 75·91	18 364·54	20 246·24	22 110·77	24 022·54	18 518·05	20 022·65*
		2_{02}–3_{12}	3·20	2·93	—	13 519·27	15 020·92 20·71	16 642·85 42·63	18 331·22	20 213·33	22 077·38	23 990·71	18 483·61	—
		3_{03}–4_{13}	7·78	6·16	—	13 482·61	14 984·56 84·23	16 606·83 06·58	18 295·31	20 178·15*	22 042·97*	23 959·03	18 446·74	19 952·15
		4_{04}–5_{14}	1·84	1·24	—	13 445·95	14 947·12	16 570·55 70·13	18 259·57	20 144·02*	22 009·99	23 925·72	18 408·91	—
		5_{05}–6_{15}	3·52	2·04	12 065·45	13 403·09	14 911·98	16 535·74 33·86	18 226·33	20 109·91 09·64	—	—	18 372·50	—
		6_{06}–7_{16}	0·68	0·35	—	—	—	—	—	—	—	—	—	—
		7_{07}–8_{17}	1·08	0·50	—	—	14 854·50 53·96	16 478·76	—	—	—	—	—	—

* Denotes overlapped line.

TABLE 1 (*cont.*)

II. Δ vibronic levels

branch: C.H.K. notation	branch: our notation	rotational transition	calculated relative intensity: $\kappa = -1$	calculated relative intensity: $\kappa = -0{\cdot}386$	(0, 7, 0) band	(0, 9, 0) band	(0, 11, 0) band	(0, 13, 0) band	(0, 15, 0) band	(1, 7, 0) band
$^{co}R_{1,0}$	$^{R}R_{1,N}$	2_{21}–1_{11}	12·87	12·87	15 023·03	16 610·36*	18 256·90	20 180·90	22 008·42	18 366·43
					12·73	05·72	55·82	78·41*	00·04	
		3_{22}–2_{12}	3·98	3·98	15 043·13	16 629·26	18 273·54	20 200·02	—	18 391·39
					36·01	26·15	72·90	198·75		
		4_{23}–3_{13}	10·31	9·96	15 069·01	16 648·71	18 292·63	20 221·10	22 045·90	18 419·68
					62·97	46·00	92·11	19·81	42·97*	
		5_{24}–4_{14}	2·71	2·48	—	16 669·48	—	—	—	—
						67·57				
		6_{25}–5_{15}	5·88	5·00	15 134·12	16 699·51	18 333·88	20 253·18	22 090·57	18 471·87
					33·20	97·10		52·08		71·25
$^{ce}R_{1,0}$	$^{R}R_{1,N-1}$	2_{20}–1_{10}	4·19	4·85	15 017·85	16 605·30	18 252·12	20 176·08	—	18 362·36
					07·69	00·78	50·89	73·34		
		3_{21}–2_{11}	11·16	15·54	15 026·93	16 613·88	18 261·24	20 185·00	22 016·30	18 368·85
					19·88	10·36	60·92	83·47	10·87	
		4_{22}–3_{12}	3·00	4·72	15 034·07	16 618·93	—	20 188·59	—	—
					28·78	16·02				
		5_{23}–4_{13}	6·53	10·74	15 041·18	16 622·26	18 264·38	20 190·27	22 030·54	18 376·81
					36·39	19·58				
$^{co}Q_{1,\bar{2}}$	$^{R}Q_{1,N}$	2_{20}–2_{12}	1·99	1·06	14 985·27	16 572·74*	18 219·37	20 143·80*	—	18 329·48
					74·96	68·06	18·31*	40·83		
		3_{21}–3_{13}	8·02	2·60	14 985·81	16 572·74*	18 219·91	20 143·80*	21 975·10	18 327·67
					78·69	69·18		42·38	69·76	
		4_{22}–4_{14}	2·62	0·45	—	16 574·47	18 218·60	20 144·02*	—	—
						71·43	18·31			
		5_{23}–5_{15}	6·47	0·58	14 997·51	16 578·54	18 220·63	20 146·50	21 986·81	18 333·05
					92·58	75·75				
		6_{24}–6_{16}	1·56	0·07	—	16 583·67	—	—	—	—
						81·01				
		7_{25}–7_{17}	3·04	0·09	—	16 593·08	—	—	—	—
						90·47				
$^{ce}Q_{1,0}$	$^{R}Q_{1,N-1}$	2_{21}–2_{11}	5·58	5·58	14 971·29	16 558·56	18 205·14	20 129·10	21 956·76	18 314·70
					60·96	53·96	04·04	26·89	48·30	
		3_{22}–3_{12}	2·33	2·70	14 959·35	16 545·48	—	20 116·34	—	—
					52·31*	42·44		14·93		
		4_{23}–4_{13}	6·30	8·71	14 950·17	16 529·87	18 173·81	20 102·37	21 927·19	18 300·93
					44·23	27·25	73·30	01·00	24·15	
		5_{24}–5_{14}	1·57	2·60	—	16 514·17	—	—	—	—
						12·36				
		6_{25}–6_{15}	3·11	6·02	14 942·39	16 507·78	18 142·24	20 061·56	21 898·99	18 280·12
					41·65	05·59		60·54		79·66

* Denotes overlapped line.

TABLE 1 (*cont.*)

II. Δ vibronic levels (*cont.*)

branch			calculated relative intensity							
C.H.K. notation	our notation	rotational transition	$\kappa = -1$	$\kappa = -0{\cdot}386$	(0, 7, 0) band	(0, 9, 0) band	(0, 11, 0) band	(0, 13, 0) band	(0, 15, 0) band	(1, 7, 0) band
${}^{co}R_{\bar{1},2}$	${}^{P}R_{3,N-2}$	4_{23}–3_{31}	0·39	0·29	14 949·01	16 528·73	—	—	—	—
					43·81	26·84				
		5_{24}–4_{32}	0·20	0·14	—	—	—	—	—	—
		6_{25}–5_{33}	0·61	0·37	14 982·48	16 547·88	—	—	—	—
					82·06	45·98				
${}^{ce}R_{\bar{1},2}$	${}^{P}R_{3,N-3}$	4_{22}–3_{30}	0·13	0·12	—	—	—	—	—	—
		5_{23}–4_{31}	0·61	0·66	14 952·31*	16 533·36	—	—	—	—
					47·94	31·14				
${}^{co}Q_{\bar{1},0}$	${}^{P}Q_{3,N-2}$	3_{21}–3_{31}	2·71	2·22	14 866·04	16 452·95	—	20 024·68	—	—
					59·61	50·08		22·65		
		4_{22}–4_{32}	1·08	0·90	—	—	—	—	—	—
		5_{23}–5_{33}	2·69	2·45	14 845·94	16 426·94	—	19 995·09	—	—
					41·48	24·64				
${}^{ce}Q_{\bar{1},2}$	${}^{P}Q_{3,N-3}$	3_{22}–3_{30}	0·90	0·67	—	—	—	—	—	—
		4_{23}–4_{31}	3·20	1·97	14 861·29	16 441·04	—	20 013·91	—	18 212·59
					55·89	38·85				11·94
${}^{co}P_{\bar{1},0}$	${}^{P}P_{3,N-2}$	2_{21}–3_{31}	7·75	8·01	14 810·41	16 397·64	18 034·83*	19 968·78	21 796·39	18 154·32
					00·69	93·66	43·14	65·93	87·42	53·88
		3_{22}–4_{32}	1·79	1·95	14 781·47	16 367·61	—	19 938·93	—	—
					74·88	65·05*				
		4_{23}–5_{33}	3·42	3·83	14 754·85	16 334·62	17 978·90	19 907·49	21 732·25	18 106·06
					49·35	32·35	78·00	05·71		05·55
		5_{24}–6_{34}	0·66	0·74	—	16 299·58	—	—	—	—
						98·08				
		6_{25}–7_{35}	1·04	1·16	—	16 270·59	—	—	—	—
						68·56				
${}^{ce}P_{\bar{1},0}$	${}^{P}P_{3,N-3}$	2_{20}–3_{30}	2·58	2·70	14 809·83	16 397·27	18 044·83*	19 968·78*	—	—
					00·18	93·29	42·73	65·28		
		3_{21}–4_{31}	5·34	6·16	14 778·17	16 365·05*	18 012·87	19 936·65	21 768·02	18 120·47
					71·58	62·04	12·17	34·65	62·13	20·05
		4_{22}–5_{32}	1·11	1·43	14 743·02	16 327·93	17 972·62	19 897·52	—	—
					38·17	25·37				
		5_{23}–6_{33}	1·85	2·63	14 703·88	16 284·90	—	19 853·26	—	—
					699·35	82·53		52·91		

* Denotes overlapped line.

TABLE 1 (*cont.*)

III. Γ vibronic levels

branch			calculated relative intensity					
C.H.K. notation	our notation	rotational transition	$\kappa = -1$	$\kappa = -0{\cdot}386$	(0, 9, 0) band	(0, 11, 0) band	(0, 13, 0) band	(0, 15, 0) band
${}^{co}R_{1,0}$	${}^{R}R_{3,N-2}$	4_{41}–3_{31}	10·85	11·14	16 093·20	17 860·62	19 698·74	21 560·12
					87·88	59·33	94·23	53·42
		5_{42}–4_{32}	2·46	2·65	—	—	—	—
		6_{43}–5_{33}	4·58	5·14	16 122·41	17 888·83	19 714·41	21 577·32
					18·11	88·03	13·16	70·66
${}^{ce}R_{1,0}$	${}^{R}R_{3,N-3}$	4_{40}–3_{30}	3·61	3·72	16 093·79	—	19 699·52	—
					88·51		94·90	
		5_{41}–4_{31}	7·32	7·97	16 110·12	17 873·64	19 710·22	21 569·02
					05·93	72·34	06·64	62·61
${}^{co}Q_{1,\bar{2}}$	${}^{R}Q_{3,N-2}$	4_{40}–4_{32}	0·61	0·49	16 007·59	—	—	—
					02·19			
		5_{41}–5_{33}	2·07	1·47	16 003·72	17 767·30	19 603·78	21 462·53
					15 999·43	65·79	600·16	
${}^{ce}Q_{1,0}$	${}^{R}Q_{3,N-3}$	4_{41}–4_{31}	1·83	1·47	16 005·27	17 772·79	19 610·68	21 472·12
					15 999·83	71·29	06·38	
		5_{42}–5_{32}	0·65	0·51	—	—	—	—
		6_{43}–6_{33}	1·43	1·12	15 980·32	—	19 572·28	21 435·31
					75·97		71·13	

TABLE 1 (*cont.*)

(B) Bands involving Π, Φ vibronic levels in the upper state

I. Π vibronic levels

branch		rotational transition	calculated relative intensity		(0, 6, 0) band	(0, 8, 0) band	(0, 10, 0) band	(0, 12, 0) band	(0, 14, 0) band	(0, 18, 0) band	(1, 6, 0) band	(1, 8, 0) band
C.H.K. notation	our notation		$\kappa = -1$	$\kappa = -0{\cdot}386$								
${}^{ce}R_{1,0}$	${}^{R}R_{0,N}$	1_{10}–0_{00}	10·0	10·0	14 374·68†	15 906·51†	17 559·49†	19 393·77	21 216·73	—	17 756·78	19 227·59
					62·14	03·62	58·74	93·28†	13·62†		53·46†	26·23†
		2_{11}–1_{01}	4·52	4·52	14 386·64	15 918·88	17 577·01	19 411·31	21 234·82	—	—	—
					78·47	16·11	76·70	11·07	33·20			
		3_{12}–2_{02}	14·85	13·62	14 399·63	15 933·70	17 593·46	19 428·23	21 253·29	25 104·70	17 784·74	19 257·48
					93·47	29·30			51·90		83·41	56·87
		4_{13}–3_{03}	4·67	3·70	14 414·52	15 949·98	17 611·76	19 446·67	—	—	—	—
					09·66	47·84			21 272·50			
		5_{14}–4_{04}	11·74	7·89	14 433·24	15 969·64	17 633·31	19 471·82	21 299·40	—	17 819·88	—
					29·15	68·18		69·86	96·50		18·91	
		6_{15}–5_{05}	2·95	1·71	14 456·55	15 993·11	17 658·53	—	—	—	—	—
					53·02	92·00						
		7_{16}–6_{06}	6·07	3·10	—	16 020·58	17 687·36	19 525·56	—	—	—	—
						19·76						
${}^{ce}Q_{1,0}$	${}^{R}Q_{0,N}$	1_{11}–1_{01}	4·52	4·52	—	15 882·62	17 536·72	19 370·75	21 193·27	—	—	—
					14 342·29	79·14	35·94					
		2_{12}–2_{02}	18·56	21·44	14 350·15	15 875·38	17 530·18	19 364·48	21 186·25	25 030·88	17 730·52	19 198·01
					41·45	72·11	29·65		85·19	29·58	28·11	
		3_{13}–3_{03}	6·54	10·47	—	15 871·19	17 523·33	19 357·16	21 180·83	—	—	—
						66·34*	22·79		79·79			
		4_{14}–4_{04}	17·60	25·74	14 356·44	15 866·65	17 517·88	19 351·54	21 170·02	25 019·14	—	19 189·88
					50·84	63·69	17·38		68·95	17·94		88·04
		5_{15}–5_{05}	4·64	7·25	—	15 866·34*	17 514·40	19 347·57	—	—	—	—
						63·96	13·86					
		6_{16}–6_{06}	9·86	16·09	—	15 869·84	17 513·45	19 346·02	21 167·63	—	—	—
						68·43	12·75		67·26			
		7_{17}–7_{07}	2·11	3·55	—	—	17 516·08	—	—	—	—	—
							15·14					
${}^{co}R_{\bar{1},2}$	${}^{P}R_{2,N-1}$	3_{13}–2_{21}	0·32	0·16	—	—	—	—	—	—	—	—
		4_{14}–3_{22}	1·59	0·63	—	15 883·19	17 534·36	19 368·28	—	—	—	—
						80·57						
		5_{15}–4_{23}	0·57	0·18	—	—	—	—	—	—	—	—
		6_{16}–5_{24}	1·45	0·36	—	—	17 541·71	—	—	—	—	—
						15 897·01	41·27					
${}^{ce}R_{\bar{1},2}$	${}^{P}R_{2,N-2}$	3_{12}–2_{20}	0·95	1·16	14 344·50	15 878·53	17 538·75	—	—	—	—	—
					38·88	74·57	38·44					
		4_{13}–3_{21}	0·52	0·63	—	15 885·80	17 547·90	—	—	—	—	—
						83·97	47·64					
		5_{14}–4_{22}	1·60	1·74	14 351·50	15 887·83	17 551·74	19 390·33	—	—	—	—
					47·68	86·65	51·40	88·05				
		6_{15}–5_{23}	0·42	0·36	—	15 885·53	—	—	—	—	—	—
						84·68						
		7_{16}–6_{24}	1·05	0·65	—	15 880·85	—	19 386·30	—	—	—	—
						80·29		85·63				

* Denotes overlapped line. † Denotes satellite line.

TABLE 1 (*cont.*)

I. Π vibronic levels (*cont.*)

branch		rotational transition	calculated relative intensity		(0, 6, 0) band	(0, 8, 0) band	(0, 10, 0) band	(0, 12, 0) band	(0, 14, 0) band	(0, 18, 0) band	(1, 6, 0) band	(1, 8, 0) band
C.H.K. notation	our notation		$\kappa = -1$	$\kappa = -0{\cdot}386$								
$^{co}Q_{\bar{1}, 0}$	$^{P}Q_{2, N-1}$	2_{11}–2_{21}	1·60	1·60	14 291·94 84·11	15 824·13 21·84	17 482·38*	—	—	—	—	—
		3_{12}–3_{22}	6·18	7·14	14 282·48 76·71	817·04† 15 816·51 12·57	17 476·61 76·45	19 311·48 11·09	21 136·50 34·80	—	17 667·65 66·81	—
		4_{13}–4_{23}	1·92	2·65	14 272·83 68·35	808·55† 15 808·30 06·43	17 470·31 70·03	19 305·09	—	—	—	—
		5_{14}–5_{24}	4·46	7·38	14 263·97 60·11	800·97† 15 800·44 799·21	17 464·29 64·09	19 302·85 00·59	—	—	17 650·58	—
		6_{15}–6_{25}	1·01	1·95	—	15 793·94 93·08	17 459·76*	—	—	—	—	—
		7_{16}–7_{26}	1·82	3·98	—	15 789·93 89·37*	17 456·84*	—	—	—	—	—
$^{ce}Q_{\bar{1}, 2}$	$^{P}Q_{2, N-2}$	2_{12}–2_{20}	4·76	2·54	14 295·13 86·79	15 820·30 17·51	17 475·03	19 309·91	21 131·64 30·08	—	—	—
$^{co}P_{\bar{1}, 0}$	$^{P}P_{2, N-1}$	1_{11}–2_{21}	2·87	2·87	14 254·70 47·94	—	17 442·08* 41·63	19 276·46 76·06	21 099·00	—	—	—
		2_{12}–3_{22}	7·06	7·06	14 233·29 24·66	15 758·30 55·41	17 413·02*	19 247·80 47·23	21 069·41 68·07	—	— 17 611·39	19 081·31 80·93
		3_{13}–4_{23}	1·78	1·72	—	15 729·96 24·91	17 381·63 81·42	19 215·69 15·08	—	—	—	—
		4_{14}–5_{24}	3·65	3·33	14 187·16 81·93	15 697·38 94·70	17 348·65 48·39	19 182·44	21 001·01 20 999·35	—	—	19 020·45 19·00
		5_{15}–6_{25}	0·76	0·64	—	15 667·54 65·03	17 315·25 14·91	—	—	—	—	—
		6_{16}–7_{26}	1·29	1·02	—	15 639·13 37·98	17 282·77 82·34	—	20 937·00	—	—	—
$^{ce}P_{\bar{1}, 0}$	$^{P}P_{2\ N-2}$	1_{10}–2_{20}	8·56	9·89	14 257·37 45·44	15 789·37*	17 442·25 42·08	19 277·07 76·06	21 100·04 096·41	—	— 17 636·84	— 19 109·59
		2_{11}–3_{21}	2·29	3·19	14 222·86 15·00	755·41†* 15 755·02 52·62	17 413·02*	19 247·80 47·23	21 071·32 69·41	—	—	—
		3_{12}–4_{22}	5·00	7·86	14 184·06 78·28	718·60† 15 718·12 14·11	17 378·08	19 213·03 12·68	21 038·05 36·44	24 889·45	—	19 042·00 41·76
		4_{13}–5_{23}	1·06	1·74	14 141·21 36·65	15 676·65 74·76	17 338·68 38·45	19 173·41	—	—	—	—
		5_{14}–6_{24}	1·81	2·93	14 095·90 92·07	15 632·38 31·18	17 296·32 96·01	19 134·94 32·55	—	—	—	—
		6_{15}–7_{25}	0·31	0·47	—	15 587·67 86·85	17 253·51 53·06	—	—	—	—	—
		7_{16}–8_{26}	0·44	0·61	—	15 545·26 44·75	—	—	—	—	—	—

* Denotes overlapped line. † Denotes satellite line.

TABLE 1 (*cont.*)

II. Φ vibronic levels

branch: C.H.K. notation	branch: our notation	rotational transition	calculated relative intensity: $\kappa = -1$	calculated relative intensity: $\kappa = -0.386$	(0, 8, 0) band	(0, 10, 0) band	(0, 12, 0) band	(0, 14, 0) band	(1, 6, 0) band
${}^{co}R_{1,0}$	${}^{R}R_{2,N-1}$	3_{31}–2_{21}	4·79	4·95	15 604·74	17 204·44	—	—	—
					595·14	03·13			
		4_{32}–3_{22}	11·13	12·09	15 622·11	17 217·65	19 080·47	20 906·21	17 361·93
					14·57	16·28	79·72*	898·40	54·31
		5_{33}–4_{23}	2·65	2·97	—	17 230·63	19 094·60	—	—
						29·12	93·49		
		6_{34}–5_{24}	5·22	5·89	15 653·06	17 245·02	19 109·59	—	—
					47·87	43·36	08·24		
${}^{ce}R_{1,0}$	${}^{R}R_{2,N-2}$	3_{30}–2_{20}	14·27	14·95	15 603·36	17 203·13	19 066·38	20 891·41	17 335·70
					593·73	01·82	65·61	84·82	28·71
		4_{31}–3_{21}	3·61	4·16	15 614·86	17 211·43	19 076·06	—	—
					07·18	10·09	75·03		
		5_{32}–4_{22}	7·46	9·59	15 625·25	17 213·73	19 079·72*	—	—
					18·50	12·47	78·72		17 339·82
${}^{co}Q_{1,\bar{2}}$	${}^{R}Q_{2,N-1}$	3_{30}–3_{22}	3·71	2·75	15 541·38	17 141·09	19 004·39	20 829·18	17 273·74
					31·63	39·65	03·48	22·69	66·58
		4_{31}–4_{23}	1·49	0·92	15 537·42	17 133·94	18 998·34	—	—
					29·65	32·50	97·47		
		5_{32}–5_{24}	3·83	1·80	15 537·85	17 126·31	18 992·48	—	17 256·61
					31·06	25·04	91·27		52·39
${}^{ce}Q_{1,0}$	${}^{R}Q_{2,N-2}$	3_{31}–3_{21}	1·20	0·99	15 535·65	—	—	—	—
					25·96				
		4_{32}–4_{22}	4·20	3·52	15 523·75	17 119·22	18 982·06	20 807·73	17 263·46
					16·15	17·85	81·22	799·91	55·95
		5_{33}–5_{23}	1·11	1·01	—	—	—	—	—
		6_{34}–6_{24}	2·16	2·27	—	17 076·98	18 941·50	—	—
						75·31	40·23		
${}^{co}Q_{\bar{1},0}$	${}^{P}Q_{4,N-3}$	4_{31}–4_{41}	0·41	0·33	—	—	—	—	—
		5_{32}–5_{42}	1·32	1·04	15 376·07	16 963·90	18 829·99	—	17 094·91
					69·85				
${}^{ce}Q_{\bar{1},2}$	${}^{P}Q_{4,N-4}$	4_{32}–4_{40}	1·21	0·96	15 383·02	16 978·34	18 841·09	—	—
					76·07	77·56			
		5_{33}–5_{41}	0·44	0·32	—	—	—	—	—
		6_{34}–6_{42}	0·99	0·64	15 359·61	—	—	—	—
${}^{co}P_{\bar{1},0}$	${}^{P}P_{4,N-3}$	3_{31}–4_{41}	1·58	1·62	—	—	—	—	—
		4_{32}–5_{42}	2·89	3·11	15 274·52	16 869·98	18 732·83*	—	—
					67·48	69·20*	32·54*		17 007·36
		5_{33}–6_{43}	0·54	0·60	—	16 835·88	—	—	—
						34·87			
		6_{34}–7_{44}	0·82	0·95	15 209·01	16 800·74	—	—	—
					03·68	799·43			
${}^{ce}P_{\bar{1},0}$	${}^{P}P_{4,N-4}$	3_{30}–4_{40}	4·72	4·85	15 302·21	16 901·88	18 764·98	20 590·05	17 034·48
					293·10	01·14		84·06	28·03
		4_{31}–5_{41}	0·96	1·05	15 271·47	16 869·20*	18 732·83*	—	—
					65·64	68·54	32·54*		
		5_{32}–6_{42}	1·60	1·86	15 244·34	16 832·82	18 699·10*	—	16 963·20
					38·04	32·02	98·28		59·30

* Denotes overlapped line.

TABLE 2. VACUUM WAVE NUMBERS, VIBRATIONAL AND ROTATIONAL ASSIGNMENTS FOR LINES OF THE ND_2 ABSORPTION SPECTRUM

(A) Bands involving Σ, Δ vibronic levels in the upper state

I. Σ vibronic levels

branch			calculated relative intensity							
C.H.K. notation	our notation	rotational transition	$\kappa = -1$	$\kappa = -0{\cdot}515$	(0, 9, 0) band	(0, 11, 0) band	(0, 13, 0) band	(0, 15, 0) band	(0, 17, 0) band	(1, 9, 0) band
${}^{ce}R_{\bar{1},2}$	${}^{P}R_{1,N-1}$	2_{02}–1_{10}	4·55	2·84	—	16 022·08	17 232·01	18 596·23	19 932·78	17 368·31
		3_{03}–2_{11}	4·06	1·76	—	16 025·91*	17 235·82	18 600·12	19 936·99	—
		4_{04}–3_{12}	10·28	2·93	14 857·60*	16 027·53	17 237·03	18 602·06	19 939·21	17 372·88
						26·97*				
		5_{05}–4_{13}	5·48	1·07	14 858·24	16 026·97*	—	18 602·58	19 940·28	17 372·06
		6_{06}–5_{14}	10·45	1·52	14 857·60*	16 025·91*	17 235·14	18 602·87	—	17 370·64
						25·04				
${}^{co}Q_{\bar{1},0}$	${}^{P}Q_{1,N}$	1_{01}–1_{11}	6·89	6·89	—	—	17 215·98	18 579·95	—	—
		2_{02}–2_{12}	20·94	23·55	14 834·61	16 004·90	17 214·88	18 579·00	19 915·57*	17 351·06
					34·40	04·71				
		3_{03}–3_{13}	12·76	16·34	14 833·32*	16 003·64	17 213·59	18 577·92	19 914·80*	17 349·56
						03·34				
		4_{04}–4_{14}	27·36	38·86	14 832·72*	16 002·67	17 212·17	18 577·19*	19 914·32	17 348·00
						02·11				
		5_{05}–5_{15}	13·35	20·34	14 832·72*	16 001·51*	17 211·11	18 577·19*	19 914·80*	17 346·63
		6_{06}–6_{16}	24·17	38·57	14 833·32*	16 001·51*	17 210·72	18 578·44	19 915·57*	17 346·19
						00·67				
${}^{ce}P_{\bar{1},0}$	${}^{P}P_{1,N-1}$	0_{00}–1_{10}	9·09	9·09	14 824·48	15 994·62	17 204·64	18 568·61	19 904·97	17 341·20
		1_{01}–2_{11}	6·09	6·09	14 809·78	15 979·95	17 190·03	18 554·04	19 890·43	17 326·22
		2_{02}–3_{12}	13·70	12·80	14 792·67	15 963·06	17 173·01	18 537·17	19 873·74	17 309·21
						62·76				
		3_{03}–4_{13}	6·86	5·61	14 773·93	15 944·29	17 154·04	18 518·49	19 855·37	17 290·10
						43·86				
		4_{04}–5_{14}	12·54	8·75	—	15 924·53	17 134·02	18 499·08	19 836·20	17 269·84
						23·88				
		5_{05}–6_{15}	5·33	3·21	—	15 904·30	17 114·06	18 479·88	19 817·56	17 249·54
		6_{06}–7_{16}	8·48	4·53	—	15 885·15	17 094·45	18 462·09	19 799·31	—
						84·31				

* Denotes overlapped line.

TABLE 2 (*cont.*)

II. Δ vibronic levels

branch			calculated relative intensity					
C.H.K. notation	our notation	rotational transition	$\kappa = -1$	$\kappa = -0{\cdot}515$	(0, 11, 0) band	(0, 13, 0) band	(0, 15, 0) band	(0, 17, 0) band
${}^{co}R_{1,0}$	${}^{R}R_{1,N}$	2_{21}–1_{11}	6·89	6·89	15 928·14	—	—	—
		3_{22}–2_{12}	13·96	13·96	15 937·65	17 142·73	—	19 859·45
						42·07		
		4_{23}–3_{13}	6·84	6·65	15 947·55	—	18 496·52	—
		5_{24}–4_{14}	12·77	11·80	15 958·18	17 162·11	18 506·10	19 876·85
						61·38		
		6_{25}–5_{15}	5·66	4·91	—	—	—	—
		7_{26}–6_{16}	9·56	7·73	—	—	18 529·73	—
${}^{ce}R_{1,0}$	${}^{R}R_{1,N-1}$	2_{20}–1_{10}	13·64	15·35	15 925·95	—	18 475·37	19 847·19
		3_{21}–2_{11}	6·76	9·06	15 931·09	—	18 479·88*	—
		4_{22}–3_{12}	12·85	19·70	15 934·58	—	18 482·50*	—
		5_{23}–4_{13}	5·76	9·44	—	—	—	—
		6_{24}–5_{14}	9·75	15·98	—	—	18 482·50*	—
${}^{co}Q_{1,\bar{2}}$	${}^{R}Q_{1,N}$	2_{20}–2_{12}	6·98	4·36	15 908·83*	—	18 458·15*	19 830·03
		3_{21}–3_{13}	5·32	2·18	15 908·83*	—	18 457·66*	19 825·35
		4_{22}–4_{14}	12·31	2·94	15 909·73	—	18 457·66*	—
		5_{23}–5_{15}	6·23	0·86	15 911·32	—	—	—
		6_{24}–6_{16}	11·51	1·01	15 913·84	—	18 458·15*	—
${}^{ce}Q_{1,0}$	${}^{R}Q_{1,N-1}$	2_{21}–2_{11}	3·38	3·38	—	—	—	—
		3_{22}–3_{12}	9·99	11·12	15 895·82	—	—	19 817·56
						17 100·26		
		4_{23}–4_{13}	5·55	7·13	15 888·19	—	18 436·93	—
		5_{24}–5_{14}	10·73	16·27	15 880·09	17 083·86	18 427·96	19 798·76
						83·33		
		6_{25}–6_{15}	4·72	8·44	15 871·99	—	—	—
		7_{26}–7_{16}	7·66	15·77	15 864·85	17 067·73	18 413·36	—
						67·09		
${}^{co}P_{\bar{1},0}$	${}^{P}P_{3\ N-2}$	2_{21}–3_{31}	6·51	6·69	—	—	—	—
		3_{22}–4_{32}	11·08	11·91	—	—	18 344·71	19 716·62
							44·13	
${}^{ce}P_{\bar{1},0}$	${}^{P}P_{3,N-3}$	2_{20}–3_{30}	13·03	13·48	15 809·84	—	18 359·21	19 731·10
		3_{21}–4_{31}	5·53	6·14	—	—	18 343·11	19 710·63

* Denotes overlapped line.

TABLE 2 (*cont.*)

(B) Bands involving Π, Φ vibronic levels in the upper state

I. Π vibronic levels

branch			calculated relative intensity				
C.H.K. notation	our notation	rotational transition	$\kappa = -1$	$\kappa = -0{\cdot}515$	(0, 10, 0) band	(0, 12, 0) band	(0, 14, 0) band
${}^{ce}R_{1\ 0}$	${}^{R}R_{0,\ N}$	1_{10}–0_{00}	5·00	5·00	—	16 604·97	17 948·55
		2_{11}–1_{01}	14·24	14·24	15 411·52	16 616·58	17 958·68
					11·13	14·77	57·15
		3_{12}–2_{02}	8·58	8·02	—	—	17 966·94
						16 622·37	65·01
		4_{13}–3_{03}	18·52	15·17	15 424·96	16 630·81	17 973·95
					23·18	29·87	71·95
		5_{14}–4_{04}	9·20	6·42	—	—	—
		6_{15}–5_{05}	17·06	10·28	—	16 649·07	—
					15 438·73	48·69	17 984·50
${}^{ce}Q_{1,\ 0}$	${}^{R}Q_{0,\ N}$	1_{11}–1_{01}	14·24	14·24	15 392·73	16 594·99	17 939·84
					91·93	93·40	37·12
		2_{12}–2_{02}	10·73	12·07	15 391·06	—	17 936·21
					88·38		34·45
		3_{13}–3_{03}	25·93	33·20	15 390·13	16 585·81	17 931·83
					86·87	85·20	
		4_{14}–4_{04}	13·80	19·60	15 386·08*	—	17 925·83
							24·39
		5_{15}–5_{05}	26·81	40·86	15 386·08*	16 579·77	—
						79·01	
${}^{ce}R_{\bar{1}\ 2}$	${}^{P}R_{2,\ N-2}$	3_{12}–2_{20}	0·61	0·75	—	—	—
		4_{13}–3_{21}	2·34	3·16	15 389·04	16 594·99	17 937·77
						94·41	
${}^{co}Q_{\bar{1},\ 0}$	${}^{P}Q_{2,\ N-1}$	2_{11}–2_{21}	6·13	6·13	15 358·34	16 563·06	17 905·34
					57·69	61·58	04·01
		3_{12}–3_{22}	4·59	5·11	—	16 558·98	17 902·29
						57·96	00·61
		4_{13}–4_{23}	10·39	13·34	15 348·39	16 554·10	17 897·20
					46·71	53·30	95·25
		5_{14}–5_{24}	5·13	7·78	—	—	—
		6_{15}–6_{25}	9·13	16·36	15 334·10	—	—
						16 544·07	
${}^{ce}Q_{\bar{1},\ 2}$	${}^{P}Q_{2,\ N-2}$	2_{12}–2_{20}	3·06	1·91	—	—	—
		3_{13}–3_{21}	9·09	3·73	—	16 549·67	17 895·97

* Denotes overlapped line.

TABLE 2 (*cont.*)

I. Π vibronic levels (*cont.*)

branch			calculated relative intensity				
C.H.K. notation	our notation	rotational transition	$\kappa = -1$	$\kappa = -0{\cdot}515$	(0, 10, 0) band	(0, 12, 0) band	(0, 14, 0) band
${}^{co}P_{\bar{1},0}$	${}^{P}P_{2,N-1}$	1_{11}–2_{21}	11·03	11·03	15 339·53	16 541·71	17 886·47
					38·93	40·12	84·03
		2_{12}–3_{22}	5·25	5·25	15 326·61	—	17 871·59
					23·88		70·06
		3_{13}–4_{23}	9·62	9·35	15 313·66	16 509·10	17 855·37
					10·26	08·65	53·99
		4_{14}–5_{24}	4·20	3·88	—	—	—
		5_{15}–6_{25}	6·89	5·97	15 281·30	16 474·96	—
						74·24	
${}^{ce}P_{\bar{1},0}$	${}^{P}P_{2,N-2}$	1_{10}–2_{20}	5·50	6·19	15 341·12	16 540·12	17 884·03
					40·62		
		2_{11}–3_{21}	10·39	13·91	15 323·88	16 528·69	17 870·85
					23·32	27·12	69·56
		3_{12}–4_{22}	4·68	7·18	15 304·04	16 510·51	17 853·99
							52·10
		4_{13}–5_{23}	7·91	12·97	15 283·90	16 489·62	17 832·62
					81·97	88·79	30·76
		5_{14}–6_{24}	3·12	5·12	—	—	—
		6_{15}–7_{25}	4·63	7·18	15 232·39	16 442·46	17 780·30

II. Φ vibronic levels

branch			calculated relative intensity		
C.H.K. notation	our notation	rotational transition	$\kappa = -1$	$\kappa = -0{\cdot}515$	(0, 14, 0) band
${}^{co}R_{1,0}$	${}^{R}R_{2,N-1}$	3_{31}–2_{21}	18·39	18·90	17 790·33
					88·90
		4_{32}–3_{22}	8·27	8·88	17 799·01
		5_{33}–4_{23}	14·37	15·94	17 812·08
${}^{ce}Q_{1,0}$	${}^{R}Q_{2,N-2}$	3_{31}–3_{21}	5·45	4·64	17 755·68
					54·48
		4_{32}–4_{22}	3·93	3·32	17 750·51
		5_{33}–5_{23}	8·29	7·23	17 747·50

TABLE 3. ISOTOPE FACTORS ($\Delta\nu/\nu$) FOR $^{14}NH_2$ AND $^{15}NH_2$

A. Assuming $k_1 = 6{\cdot}0 \times 10^5$ dyn/cm and $k_\delta/l^2 = 0{\cdot}6 \times 10^5$ dyn/cm

apex angle	$\Delta\nu_1/\nu_1$	$\Delta\nu_2/\nu_2$	$\Delta\nu_3/\nu_3$
180°	0·00000	0·00419	0·00419
150°	0·00034	0·00385	0·00394
120°	0·00121	0·00298	0·00324
90°	0·00230	0·00189	0·00223

B. Assuming $k_1 = 6{\cdot}564 \times 10^5$ dyn/cm and $k_\delta/l^2 = 0{\cdot}1004 \times 10^5$ dyn/cm

apex angle	$\Delta\nu_1/\nu_1$	$\Delta\nu_2/\nu_2$	$\Delta\nu_3/\nu_3$
180°	0·00000	0·00419	0·00419
150°	0·00032	0·00387	0·00394
120°	0·00116	0·00303	0·00324
90°	0·00224	0·00195	0·00223

TABLE 4. TYPICAL GROUND-STATE COMBINATION DIFFERENCES OBTAINED FROM VARIOUS BANDS IN THE NH_2 ABSORPTION SPECTRUM

A. Differences obtained from Σ vibronic sub-bands

ground-state difference	upper-state vibrational level (0, 3, 0)	(0, 5, 0)	(0, 7, 0)	(0, 9, 0)	(0, 11, 0)	(0, 13, 0)	(0, 15, 0)	(0, 17, 0)	(1, 7, 0)
$2_{11}-1_{11}$	51·81	51·77	51·77	51·75	51·93	51·76	51·84	51·87	51·88
			51·73	51·66	51·66				
$3_{12}-2_{12}$	—	83·78	83·75	83·65	83·68	83·63	83·74	83·73	83·79
			83·81	83·87					
$4_{13}-2_{11}$	—	159·94	159·92	159·92	159·94	159·94	159·96	159·93	159·92
			159·93	159·95					
$5_{14}-3_{12}$	—	199·91	199·84	199·78	199·71	199·92	199·83	—	199·79
				199·82	200·07	199·92			
$6_{15}-4_{13}$	—	235·29	235·37	235·42	235·41	235·28	—	—	235·40
				235·34		235·55			

B. Differences obtained from Π vibronic sub-bands

ground state difference	upper-state vibrational level (0, 6, 0)	(0, 8, 0)	(0, 10, 0)	(0, 12, 0)	(0, 14, 0)	(0, 18, 0)	(1, 6, 0)	(1, 8, 0)
$2_{20}-0_{00}$	117·31	117·14	117·24	116·70	116·69	—	—	—
	116·70	—	116·66	117·22	117·21	—	116·62	116·64
$3_{21}-1_{01}$	163·78	163·86	163·99	163·51	163·50	—	—	—
	163·47	163·49	163·68	163·84	163·79	—	—	—
$4_{22}-2_{02}$	215·57	215·58	215·38	215·20	215·24	215·25	—	215·48
	215·19	215·19		215·55	215·46	—	—	215·11
$5_{23}-3_{03}$	273·31	273·33	273·08	273·26	—	—	—	—
	273·01	273·08	273·31	—	273·15	—	—	—
$6_{24}-4_{04}$	337·34	337·26	336·99	336·88	—	—	337·50*	—
	337·08	337·00	337·30	337·31	—	—	—	—

(Units: cm^{-1}.)

* Derived using an overlapped line.

TABLE 5. SUMMARY OF MOLECULAR CONSTANTS FOR NH_2 AND ND_2

state	constant	NH_2	ND_2	unit
$X\ ^2B_1$	A_{000}	$23{\cdot}72_8$	13·33	cm^{-1}
	B_{000}	$12{\cdot}94_2$	6·49	cm^{-1}
	C_{000}	$8{\cdot}16_9$	4·30	cm^{-1}
	D_A	$0{\cdot}019_4$	0·007	cm^{-1}
	D_B	$0{\cdot}002_0$	0·000	cm^{-1}
	D_C	0·000	0·001	cm^{-1}
	I_A	$1{\cdot}179_6$	2·100	10^{-40} g cm^2
	I_B	$2{\cdot}162_6$	$4{\cdot}31_3$	10^{-40} g cm^2
	I_C	$3{\cdot}425_8$	$6{\cdot}50_9$	10^{-40} g cm^2
	$\Delta\ (=I_C-I_A-I_B)$	$0{\cdot}083_6$	$0{\cdot}09_6$	10^{-40} g cm^2
	r_{000} (NH)	1·024	1·024	Å
	angle	103° 23′	103° 16′	
$A\ ^2A_1\Pi_u$	B_{000}	$8{\cdot}7_8$	$4{\cdot}4_1$	cm^{-1}
	α_1	0·12	—	cm^{-1}
	α_2	−0·024	−0·011	cm^{-1}
	I_{000}	$3{\cdot}1_8$	$6{\cdot}3_5$	10^{-40} g cm^2
	r_{000} (NH)	$0{\cdot}97_6$	$0{\cdot}97_4$	Å
	angle	180°	180°	
	$\omega_1^0+x_{11}^0$	3325	∼ 2520	cm^{-1}
	x_{12}^0	5	—	cm^{-1}
	ω_2^0	622	422	cm^{-1}
	x_{22}^0	$11{\cdot}_4$	$8{\cdot}_1$	cm^{-1}
	T_{000}	10249	10393	cm^{-1}

TABLE 6. GROUND-STATE ROTATIONAL TERM VALUES FOR NH_2

level	experimental term values for the two spin components		spin splitting	calculated mean term value neglecting centrifugal distortion*	centrifugal distortion correction for NH_2	centrifugal distortion correction for H_2O†
0_{00}	0·00	0·00	0·00	0·00	0·00	0·00
1_{01}	(21·11)	(21·11)	(0·00)	21·11	(0·00)	0·00
1_{11}	(31·87)	(31·87)	(0·00)	31·90	(0·03)	0·03
1_{10}	(36·65)	(36·65)	0·00	36·67	(0·02)	0·02
2_{02}	62·11	62·04	0·07	62·07	0·00	0·05
2_{12}	69·41	69·20	0·21	69·34	0·04	0·04
2_{11}	83·63	83·63	0·00	83·66	0·03	0·04
2_{21}	115·79	115·43	0·36	116·02	0·41	0·41
2_{20}	117·22	116·67	0·55	117·29	0·35	0·40
3_{03}	120·78	120·73	0·05	120·83	0·07	0·16
3_{13}	124·80	124·74	0·06	124·81	0·04	0·11
3_{12}	153·14	153·08	0·06	153·23	0·12	0·18
3_{22}	179·23	178·78	0·45	179·35	0·35	0·40
3_{21}	184·93	184·60	0·33	185·19	0·42	0·42
3_{31}	244·53	243·93	0·60	245·92	1·69	2·06
3_{30}	244·71	244·15	0·56	246·14	1·71	2·06
4_{04}	195·83	195·73	0·10	195·86	0·08	0·34
4_{14}	197·71	197·54	0·17	197·70	0·07	0·26
4_{13}	243·63	243·52	0·11	243·96	0·39	0·54
4_{23}	262·48	262·17	0·31	262·79	0·47	0·56
4_{22}	277·64	277·24	0·40	278·01	0·57	0·71
4_{32}	331·07	330·31	0·76	332·37	1·68	2·01
4_{31}	332·41	331·96	0·45	333·84	1·66	2·01
4_{41}	(418·51)	(417·32)	(1·19)	422·86	(4·94)	6·44
4_{40}	418·54	417·35	1·19	422·89	4·94	6·44
5_{05}	(286·57)	(286·45)	(0·12)	286·77	(0·26)	0·58
5_{15}	287·35	287·24	0·11	287·53	0·24	0·51
5_{14}	353·02	352·91	0·11	353·75	0·79	1·17
5_{24}	365·08	364·72	0·36	365·55	0·65	0·87
5_{23}	394·10	393·79	0·31	395·16	1·22	1·39
5_{33}	438·92	438·39	0·53	440·49	1·84	2·22
5_{32}	444·17	443·73	0·44	445·85	1·90	2·31
5_{42}	526·86	525·90	0·96	531·21	4·83	6·31
5_{41}	527·06	526·17	0·89	531·48	4·86	6·31
5_{51}	—	—	—	647·18	—	15·42
5_{50}	—	—	—	647·18	—	15·42
6_{06}	(393·43)	(393·31)	(0·12)	393·70	(0·33)	0·95
6_{16}	393·79	393·59	0·20	393·99	0·30	0·89
6_{15}	479·03	478·84	0·19	480·41	1·47	2·00
6_{25}	485·73	485·38	0·35	486·77	1·22	1·58
6_{24}	533·14	532·72	0·42	535·10	2·17	2·75
6_{34}	567·61	567·03	0·58	569·78	2·46	2·92
6_{33}	580·97	580·55	0·42	583·55	2·79	3·32
6_{43}	657·23	656·42	0·81	661·87	5·05	6·47
6_{42}	658·55	657·69	0·86	663·17	5·05	6·48
6_{52}	—	—	—	777·10	—	14·92
6_{51}	—	—	—	777·14	—	14·92
6_{61}	—	—	—	918·94	—	31·16
6_{60}	—	—	—	918·94	—	31·16
7_{07}	—	—	—	516·81	—	1·46
7_{17}	516·23	516·04	0·19	516·91	0·78	1·45
7_{16}	—	—	—	622·66	—	3·05
7_{26}	624·12	623·74	0·38	625·69	1·76	2·55
7_{25}	692·01	691·59	0·42	695·63	3·83	4·93
7_{35}	716·27	715·78	0·49	719·48	3·46	4·20
7_{34}	—	—	—	747·11	—	5·37
7_{44}	—	—	—	814·84	—	7·36
7_{43}	—	—	—	819·19	—	7·30
7_{53}	—	—	—	929·44	—	14·98
7_{52}	—	—	—	929·69	—	14·95
7_{62}	—	—	—	1070·38	—	30·20
7_{61}	—	—	—	1070·39	—	30·20
7_{71}	—	—	—	1238·16	—	55·86
7_{70}	—	—	—	1238·16	—	55·86

Units: cm^{-1}. Numbers in parentheses denote assumed values.

* Assuming $A = 23{\cdot}728\ cm^{-1}$, $B = 12{\cdot}942\ cm^{-1}$, $C = 8{\cdot}169\ cm^{-1}$.

† From Benedict & Plyler (1951).

TABLE 7. GROUND-STATE ROTATIONAL TERM VALUES FOR ND_2

level	experimental term values for the two spin components		spin splitting	calculated mean term value neglecting centrifugal distortion*	centrifugal distortion correction for ND_2	centrifugal distortion correction for D_2O†
0_{00}	0·00	0·00	0·00	0·00	0·00	0·00
1_{01}	(10·78)	(10·78)	(0·00)	10·79	(0·01)	0·01
1_{11}	(17·63)	(17·63)	(0·00)	17·63	(0·00)	0·00
1_{10}	(19·80)	(19·80)	(0·00)	19·82	(0·02)	0·02
2_{02}	(31·87)	(31·87)	(0·00)	31·92	(0·05)	0·05
2_{12}	36·99	36·99	0·00	37·02	0·03	0·02
2_{11}	43·56	43·56	0·00	43·59	0·03	0·04
2_{21}	64·14	63·93	0·21	64·11	0·07	0·06
2_{20}	64·62	64·42	(0·20)	64·56	0·04	0·04
3_{03}	62·54	62·50	(0·04)	62·62	0·10	0·13
3_{13}	65·80	65·76	(0·04)	65·85	0·07	0·03
3_{12}	78·88	78·80	(0·08)	78·93	0·09	0·08
3_{22}	96·46	96·28	0·18	96·48	0·11	0·09
3_{21}	98·62	98·41	0·21	98·60	0·09	0·06
3_{31}	—	—	—	136·41	—	0·33
3_{30}	136·02	135·82	(0·20)	136·47	0·55	0·35
4_{04}	(102·00)	(101·92)	(0·08)	102·11	(0·15)	0·19
4_{14}	103·75	103·67	0·08	103·88	0·17	0·20
4_{13}	125·29	125·16	0·13	125·36	0·13	0·32
4_{23}	139·21	139·02	0·19	139·29	0·17	0·05
4_{22}	144·90	144·70	(0·20)	145·07	0·27	0·15
4_{32}	179·82	179·74	0·08	180·31	0·53	0·38
4_{31}	180·52	180·31	0·21	180·72	0·31	0·36
4_{41}	—	—	—	235·21	—	1·57
4_{40}	—	—	—	235·22	—	1·57
5_{05}	(149·88)	(149·76)	(0·12)	150·03	(0·21)	0·30
5_{15}	150·74	150·61	0·13	150·91	0·23	0·30
5_{14}	181·94	181·78	0·16	182·23	0·37	0·54
5_{24}	—	—	—	192·25	—	0·27
5_{23}	203·75	203·58	0·17	204·00	0·34	0·39
6_{06}	—	—	—	206·35	—	0·39
6_{16}	206·33	206·17	0·16	206·75	0·50	0·38
6_{15}	247·99	247·86	0·13	248·58	0·66	0·68
6_{25}	254·67	254·38	0·29	255·03	0·50	0·50
6_{24}	—	—	—	274·99	—	0·77
7_{07}	—	—	—	271·14	—	0·43
7_{17}	—	—	—	271·31	—	0·43
7_{16}	322·68	322·52	0·16	323·58	0·98	0·79
7_{26}	—	—	—	327·31	—	0·71
7_{25}	356·38	355·99	0·39	357·33	1·14	1·07

Units: cm^{-1}. Numbers in parentheses denote assumed values.
* Assuming $A = 13{\cdot}33\ cm^{-1}$, $B = 6{\cdot}49\ cm^{-1}$, $C = 4{\cdot}30\ cm^{-1}$.
† Calculated from data given by Benedict *et al.* (1956).

TABLE 8. EXPERIMENTALLY DETERMINED ROTATIONAL TERM VALUES FOR THE EXCITED STATE OF NH_2

(A) Σ, Δ, Γ vibronic levels

vibronic symmetry	rotational level	upper-state vibrational level (0, 3, 0)	(0, 5, 0)	(0, 7, 0)	(0, 9, 0)	(0, 11, 0)	(0, 13, 0)	(0, 15, 0)	(0, 17, 0)	(1, 7, 0)	(1, 9, 0)
Σ	0_{00}	—	13 618·89	15 120·19	16 741·70	18 430·23	20 311·69	22 175·91	—	18 583·93	—
	1_{01}	12 298·78	13 636·70	15 138·12	16 759·71	18 448·19	20 329·87	22 194·44	24 106·23	18 601·78	20 106·36
				137·92	759·49						
	2_{02}	12 336·16	13 672·39	15 174·06	16 795·96	18 484·43	20 366·43	22 230·49	24 143·76	18 636·71	—
				173·75	795·69						
	3_{03}	12 386·01	13 726·17	15 228·13	16 850·46	18 538·88	20 421·72	22 286·56	24 202·60	18 690·29	20 195·69
				227·78	850·16						
	4_{04}	—	13 798·96	15 300·09	16 923·48	18 612·50	20 497·43	22 362·93	24 278·68	18 761·24	—
					923·03						
	5_{05}	12 544·36	13 882·01	15 390·95	17 014·83	18 705·30	20 588·74	22 461·64	—	18 851·45	—
					012·72						
	6_{06}	—	—	15 500·75	17 125·74	18 817·71	20 703·11	22 583·84	—	18 960·08	—
					125·08						
	7_{07}	—	—	15 631·89	17 256·03	18 949·55	20 838·89	—	—	—	—
				631·08							
$\Delta^{(+)}$	2_{20}	—	—	15 054·50	16 641·96	18 288·78	20 212·80	—	—	18 398·89	—
				044·35	637·45	287·50	210·00				
	3_{21}	—	—	15 110·57	16 697·47	18 344·85	20 268·61	22 099·94	—	18 452·45	—
				103·52	694·00	344·57	267·12	094·51			
	4_{22}	—	—	15 187·20	16 772·06	18 416·33	20 341·70	—	—	—	—
				181·88	769·11	415·85					
	5_{23}	—	—	15 284·84	16 865·88	18 507·94	20 433·81	22 274·11	—	18 620·36	—
				279·87	863·05						
$\Delta^{(-)}$	2_{21}	—	—	15 054·92	16 642·19	18 288·77	20 212·74	22 040·33	—	18 398·32	—
				044·60	637·59	287·68	210·49	031·93			
	3_{22}	—	—	15 112·52	16 698·67	18 342·74	20 269·24	—	—	18 460·69	
				105·21	695·37	342·31	268·11				
	4_{23}	—	—	15 193·79	16 773·50	18 417·33	20 345·87	22 170·66	—	18 544·46	—
				187·73	770·76	416·92	344·62	167·77			
	5_{24}	—	—	—	16 867·19	—	—	—	—	—	—
					865·12						
	6_{25}	—	—	15 421·44	16 986·83	18 621·18	20 540·41	22 377·90	—	18 759·18	—
				420·46	984·38		539·50			758·49	
$\Gamma^{(+)}$	4_{40}	—	—	—	16 338·58	—	19 943·57	—	—	—	—
					332·58		939·61				
	5_{41}	—	—	—	16 442·58	18 206·13	20 042·17	21 900·98	—	—	—
					437·85	204·24	039·06	895·02			
$\Gamma^{(-)}$	4_{41}	—	—	—	16 337·70	18 105·17	19 942·65	21 804·06	—	—	—
					331·80	103·25	938·77	797·95			
	5_{42}	—	—	—	—	—	—	—	—	—	—
	6_{43}	—	—	—	16 561·31	—	20 152·81	22 015·78	—	—	—
					556·51		152·09	009·58			

TABLE 8 (*cont.*)

(B) Π, Φ vibronic levels

vibronic symmetry	rotational level	upper-state vibrational level (0, 6, 0)	(0, 8, 0)	(0, 10, 0)	(0, 12, 0)	(0, 14, 0)	(0, 18, 0)	(1, 6, 0)	(1, 8, 0)
$\Pi^{(+)}$	1_{10}	14 374·53	15 906·51	17 559·48	19 393·75	21 216·72	—	17 756·78	19 227·59
		362·13	903·62	558·74	393·28	213·62		753·48	226·24
	2_{11}	14 407·76	15 939·95	17 598·12	19 432·41	21 255·92	—	—	—
		399·57	937·24	597·81	432·17	254·32			
	3_{12}	14 461·72	15 995·77	17 655·70	19 490·30	21 315·30	25 166·83	17 846·86	19 319·61
		455·51	991·35	655·35		314·04		845·52	318·95
	4_{13}	14 535·31	16 070·76	17 732·51	19 567·28	21 393·18	—	—	—
		530·45	068·57						
	5_{14}	14 629·05	16 165·50	17 829·10	19 667·59	21 495·13	—	18 015·69	—
		624·83	163·91		665·68	492·33		014·64	
	6_{15}	14 743·12	16 279·68	17 945·07	—	—	—	—	—
		739·47	278·45						
	7_{16}	—	16 414·03	18 080·76	—	—	—	—	—
			413·07						
$\Pi^{(-)}$	1_{11}	14 370·49	15 903·73	17 557·85	19 391·87	21 214·40	—	—	—
		363·38	900·25	557·05					
	2_{12}	14 412·26	15 937·51	17 592·27	19 426·53	21 248·24	25 092·92	17 792·63	19 260·54
		403·46	934·17	591·76		247·30	091·69	790·16	259·71
	3_{13}	—	15 992·44	17 644·11	19 477·71	21 301·56	—	—	—
			987·08	643·55		300·57			
	4_{14}	14 552·25	16 062·47	17 713·72	19 547·33	21 365·74	25 214·87	—	19 385·62
		546·61	059·42	713·11		364·60	213·77		383·74
	5_{15}	—	16 153·27	17 800·97	19 634·08	—	—	—	—
			150·41	800·30					
	6_{16}	—	16 263·25	17 906·88	—	—	—	—	—
			261·73	906·07					
$\Phi^{(+)}$	3_{30}	—	15 720·65	17 320·36	19 183·59	21 008·60	—	17 452·97	—
			710·42	318·47	182·29	001·47		445·37	
	4_{31}	—	15 799·98	17 396·39	19 260·91	—	—	—	—
			791·80	394·69	259·62				
	5_{32}	—	15 902·91	17 491·38	19 357·46	—	—	17 621·72	—
			895·76	489·72	355·97			617·05	
$\Phi^{(-)}$	3_{31}	—	15 720·55	17 320·23	—	—	—	—	—
			710·57	318·48					
	4_{32}	—	15 801·37	17 396·86	19 259·70	21 085·41	—	17 541·13	—
			793·37	395·08	258·47	077·17		533·18	
	5_{33}	—	—	17 493·11	19 357·08	—	—	—	—
				491·29	355·66				
	6_{34}	—	16 018·14	17 610·11	19 474·65	—	—	—	—
			012·59	608·06	472·95				

TABLE 9. EXPERIMENTALLY DETERMINED ROTATIONAL TERM VALUES FOR THE EXCITED STATE OF ND_2

(A) Σ, Δ vibronic levels

vibronic symmetry	rotational level	upper-state vibrational level (0, 9, 0)	(0, 11, 0)	(0, 13, 0)	(0, 15, 0)	(0, 17, 0)	(1, 9, 0)
Σ	0_{00}	14 844·28	16 014·42	17 224·44	18 588·41	19 924·77	17 361·00
	1_{01}	14 853·34	16 023·51	17 233·60	18 597·59	19 933·99	17 369·78
	2_{02}	14 871·51	16 041·90	17 251·85	18 616·02	19 952·58	17 388·08
			041·65				
	3_{03}	14 899·12	16 069·46	17 279·36	18 643·70	19 980·57	17 415·33
			069·10				
	4_{04}	14 936·45	16 106·38	17 315·88	18 680·91	20 018·05	17 451·71
			105·79				
	5_{05}	14 983·43	16 152·20	17 361·87	18 727·82	20 065·49	17 497·30
	6_{06}	15 039·51	16 207·77	17 417·01	18 784·70	20 121·86	17 552·47
			206·91				
$\Delta^{(+)}$	2_{20}	—	15 945·78	—	18 495·15	19 867·02	—
	3_{21}	—	15 974·64	—	18 523·45	19 891·08	—
	4_{22}	—	16 013·43	—	18 561·35	—	—
	5_{23}	—	16 061·99	—	—	—	—
	6_{24}	—	16 120·09	—	18 664·38	—	—
$\Delta^{(-)}$	2_{21}	—	15 945·77	—	—	—	—
	3_{22}	—	15 974·64	17 179·72	18 524·53	19 896·41	—
				179·07	523·87		
	4_{23}	—	16 013·37	—	18 562·22	—	—
	5_{24}	—	16 061·92	17 265·83	18 609·81	19 980·59	—
				265·08			
	6_{25}	—	16 119·91	—	—	—	—
	7_{26}	—	16 187·45	17 390·41	18 735·97	—	—
				389·61			

(B) Π, Φ vibronic levels

vibronic symmetry	rotational level	upper-state vibrational level (0, 10, 0)	(0, 12, 0)	(0, 14, 0)
$\Pi^{(+)}$	1_{10}	15 405·54	16 604·80	17 948·55
		405·24		
	2_{11}	15 422·29	16 627·29	17 969·47
		421·89	625·53	967·95
	3_{12}	15 448·94	16 655·42	17 998·82
		448·74	654·24	996·87
	4_{13}	15 487·45	16 693·34	18 036·42
		485·72	692·35	034·35
	5_{14}	—	16 740·93	—
			740·09	
	6_{15}	15 588·58	16 798·95	18 136·68
			798·45	134·26
$\Pi^{(-)}$	1_{11}	15 403·59	16 605·81	17 950·61
		402·89	604·11	947·93
	2_{12}	15 422·91	—	17 968·06
		420·30		966·33
	3_{13}	15 452·65	16 648·33	17 994·47
		449·44	647·68	993·01
	4_{14}	15 488·04	—	18 027·83
				026·31
	5_{15}	15 535·86	16 729·64	—
			728·69	
$\Phi^{(-)}$	3_{31}	—	—	17 854·38
				852·86
	4_{32}	—	—	17 895·35
	5_{33}	—	—	17 951·17

TABLE 10. ORIGINS OF THE VIBRONIC SUB-BANDS OF NH_2

(Units: cm^{-1}.)

vibrational level	Σ	Π	Δ	Φ	Γ	G
(0, 3, 0)	12 281·0 (12 220)	—	—	—	—	—
(0, 4, 0)	—	—	—	—	—	—
(0, 5, 0)	13 618·8_9 (13 650)	—	—	—	—	—
(0, 6, 0)	—	14 358·$_1$ (14 340)	—	—	—	—
(0, 7, 0)	15 120·0_8 (15 160)	—	15 030 (14 960)	—	—	22·$_2$
(0, 8, 0)	—	15 890·$_7$ (15 910)	—	15 685·$_5$ (15 540)	—	25·$_6$
(0, 9, 0)	16 741·7_0 (16 770)	—	16 621·$_0$ (16 610)	—	16 294·$_4$ (16 110)	28·$_5$
(0, 10, 0)	—	17 549·$_1$ (17 570)	—	17 290·$_6$ (17 280)	—	32·$_3$
(0, 11, 0)	18 430·2_3 (18 470)	—	18 269·$_8$ (18 340)	—	18 064 (17 920)	26·$_7$
(0, 12, 0)	—	19 383·$_5$ (19 320)	—	19 154 (19 070)	—	28·$_7$
(0, 13, 0)	20 311·6_9 (20 260)	—	20 192·$_7$ (20 150)	—	19 902·$_3$ (19 800)	26·$_5$
(0, 14, 0)	—	21 205·$_6$ (21 170)	—	20 976 (20 950)	—	28·$_7$
(0, 15, 0)	22 175·9_1 (22 150)	—	22 017 (22 050)	—	21 762 (21 750)	28·$_9$
(0, 16, 0)	—	—	—	—	—	—
(0, 17, 0)	24 087·8 (24 110)	—	—	—	—	—
(0, 18, 0)	—	25 050 (25 110)	—	—	—	—
(1, 6, 0)	—	17 745·$_7$	—	17 420	—	—
(1, 7, 0)	18 583·9_3	—	18 379·$_4$	—	—	—
(1, 8, 0)	—	19 215	—	—	—	—
(1, 9, 0)	20 088·5_7	—	—	—	—	—
						mean 27·6

The numbers in parentheses are the values calculated (to the nearest 10 cm^{-1}) from the Pople & Longuet-Higgins theory of the Renner effect.

TABLE 11. ORIGINS OF THE VIBRONIC SUB-BANDS OF ND_2

(Units: cm^{-1}.)

vibrational level	Σ	Π	Δ	Φ	G
(0, 9, 0)	14 844·2_8 (14 850)	—	—	—	—
(0, 10, 0)	—	15 399·$_7$ (15 400)	—	—	—
(0, 11, 0)	16 014·4_2 (16 020)	—	15 936·$_1$ (15 910)	—	19·$_6$
(0, 12, 0)	—	16 600·$_3$ (16 600)	—	—	—
(0, 13, 0)	17 224·4_4 (17 250)	—	17 141·$_1$ (17 160)	—	20·$_8$
(0, 14, 0)	—	17 944·$_4$ (17 880)	—	17 838 (17 700)	13·$_3$
(0, 15, 0)	18 588·4_1 (18 560)	—	18 485·$_6$ (18 470)	—	25·$_7$
(0, 16, 0)	—	—	—	—	—
(0, 17, 0)	19 924·7_7 (19 920)	—	19 857·$_5$ (19 850)	—	16·$_8$
(1, 9, 0)	17 361·0_0	—	—	—	—
					mean 19·2

The numbers in parentheses are the values calculated (to the nearest 10 cm^{-1}) from the Pople & Longuet-Higgins theory of the Renner effect.

TABLE 12. ROTATIONAL CONSTANTS FOR THE EXCITED STATE OF NH_2

vibrational level	B (cm^{-1}) Σ	Π	Δ	Φ	Γ	D (cm^{-1}) Σ
(0, 3, 0)	8·76 ± 0·10	—	—	—	—	—
(0, 4, 0)	—	—	—	—	—	—
(0, 5, 0)	8·90 ± 0·01	—	—	—	—	−0·003
(0, 6, 0)	—	9·5	—	—	—	—
(0, 7, 0)	8·95 ± 0·01	—	9·8	—	—	−0·003
(0, 8, 0)	—	9·2	—	10·0	—	—
(0, 9, 0)	9·01 ± 0·01	—	9·4	—	10·2	−0·003
(0, 10, 0)	—	9·2	—	9·6	—	—
(0, 11, 0)	9·03 ± 0·01	—	9·2	—	10·1	$-0·004_5$
(0, 12, 0)	—	9·2	—	9·6	—	—
(0, 13, 0)	9·09 ± 0·01	—	9·4	—	9·7	$-0·005_7$
(0, 14, 0)	—	9·2	—	9·5	—	—
(0, 15, 0)	9·02 ± 0·02	—	9·6	—	9·7	−0·016
(0, 16, 0)	—	—	—	—	—	—
(0, 17, 0)	9·17 ± 0·05	—	—	—	—	−0·024
(0, 18, 0)	—	(9·2)	—	—	—	—
(1, 6, 0)	—	9·2	—	9·5	—	—
(1, 7, 0)	8·83	—	9·6	—	—	−0·003
(1, 8, 0)	—	9·2	—	—	—	—
(1, 9, 0)	8·89	—	—	—	—	−(0·003)

Numbers in parentheses denote assumed values. The B values for the Π, Δ, Φ and Γ levels are significant to 0·1 or 0·2 cm^{-1}.

TABLE 13. ROTATIONAL CONSTANTS FOR THE EXCITED STATE OF ND_2

vibrational level	B (cm^{-1}) Σ	Π	Δ	Φ	D (cm^{-1}) Σ
(0, 9, 0)	4·52	—	—	—	−0·004
(0, 10, 0)	—	4·6	—	—	—
(0, 11, 0)	4·55	—	4·8	—	−0·001
(0, 12, 0)	—	4·6	—	—	—
(0, 13, 0)	4·56	—	4·8	—	$-0·000_5$
(0, 14, 0)	—	4·6	—	5·2	—
(0, 15, 0)	4·58	—	4·8	—	−0·002
(0, 16, 0)	—	—	—	—	—
(0, 17, 0)	4·62	—	$4·7_5$	—	−0·002
(1, 9, 0)	4·51	—	—	—	−0·001

The B values for the Σ levels are accurate to ± 0·01 cm^{-1}.
The values for the Π, Δ and Φ levels are significant to 0·1 or 0·2 cm^{-1}.

TABLE 14. OBSERVED AND CALCULATED BAND ORIGINS FOR NH_2 AND ND_2

vibrational level	NH_2			ND_2		
	ν_0 (obs.)	ν_0 (calc.)	diff.	ν_0 (obs.)	ν_0 (calc.)	diff.
(0, 3, 0)	12 281·0	12 217·8	+63·2	—	11 732·2	—
(0, 4, 0)	—	12 919·4	—	—	12 211·3	—
(0, 5, 0)	13 618·9	13 643·8	−24·9	(12 750)	12 706·6	+43
(0, 6, 0)	14 385·$_7$	14 391·0	− 5·$_3$	(13 210)	13 218·1	− 8
(0, 7, 0)	15 120·1	15 160·8	−40·7	(13 740)	13 746·0	− 6
(0, 8, 0)	15 916·$_3$	15 953·4	−37·$_1$	(14 245)	14 290·2	−45
(0, 9, 0)	16 741·7	16 768·6	−26·9	14 844·3	14 850·6	− 6·3
(0, 10, 0)	17 581·$_4$	17 606·7	−25·$_3$	15 418·$_9$	15 427·3	− 8·$_4$
(0, 11, 0)	18 430·2	18 467·4	−37·2	16 014·4	16 020·3	− 5·9
(0, 12, 0)	19 412·$_2$	19 350·8	+61·$_4$	16 619·$_5$	16 629·5	−10·$_0$
(0, 13, 0)	20 311·7	20 257·0	+53·7	17 224·4	17 255·1	−30·7
(0, 14, 0)	21 234·$_3$	21 185·9	+48·$_4$	17 957·$_7$	17 896·9	+60·$_8$
(0, 15, 0)	22 175·9	22 137·6	+38·3	18 588·4	18 555·0	+33·4
(0, 16, 0)	—	23 111·9	—	(19 250)	19 229·3	+21
(0, 17, 0)	24 087·8	24 109·0	−21·2	19 924·8	19 920·0	+ 4·8
(0, 18, 0)	25 077·$_6$	25 128·8	−51·$_2$	(20 575)	20 626·9	−52

Units: cm^{-1}. Values in parentheses are estimated from clusters of absorption lines and are not accurate to better than ± 10 cm^{-1}.

TABLE 15. EFFECTS OF FERMI RESONANCE FOR NH_2

v_2'	$\nu_0(0, v_2', 0)$ (cm^{-1})	$\nu_0(1, v_2'-4, 0)$ (cm^{-1})	difference (cm^{-1})	calculated shift due to resonance (cm^{-1})	a^2	b^2
10	17 549·$_1$	17 745·$_7$	−196·$_6$	31·4	0·84	0·16
11	18 430·2	18 583·9	−153·7	50·0	0·67	0·33
12	19 383·$_5$	19 215	+168·$_5$	40·5	0·76	0·24
13	20 311·7	20 088·6	+223·1	26·3	0·88	0·12

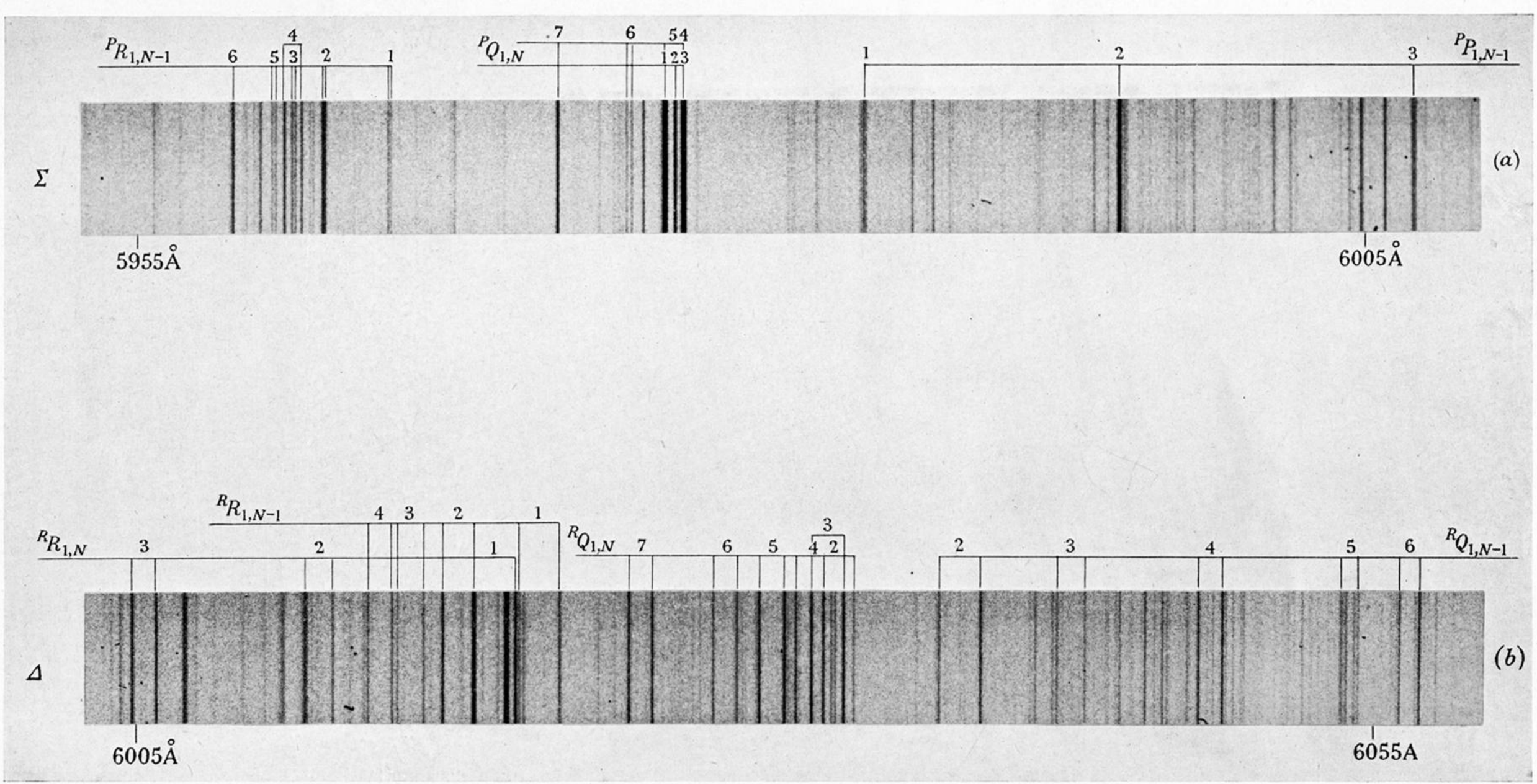

FIGURE 1. Rotational assignments for the (0, 9, 0) ← (0, 0, 0) band of NH_2. In (*a*) the three branches of the Σ vibronic sub-band are shown. The strong *Q* branch 'doublet' is the strongest feature in the absorption spectrum of NH_2. A rotational perturbation may be seen in the *R* branch. In (*b*) the strongest *R* and *Q* branches of the Δ vibronic sub-band are shown.

(*Facing p.* 554)

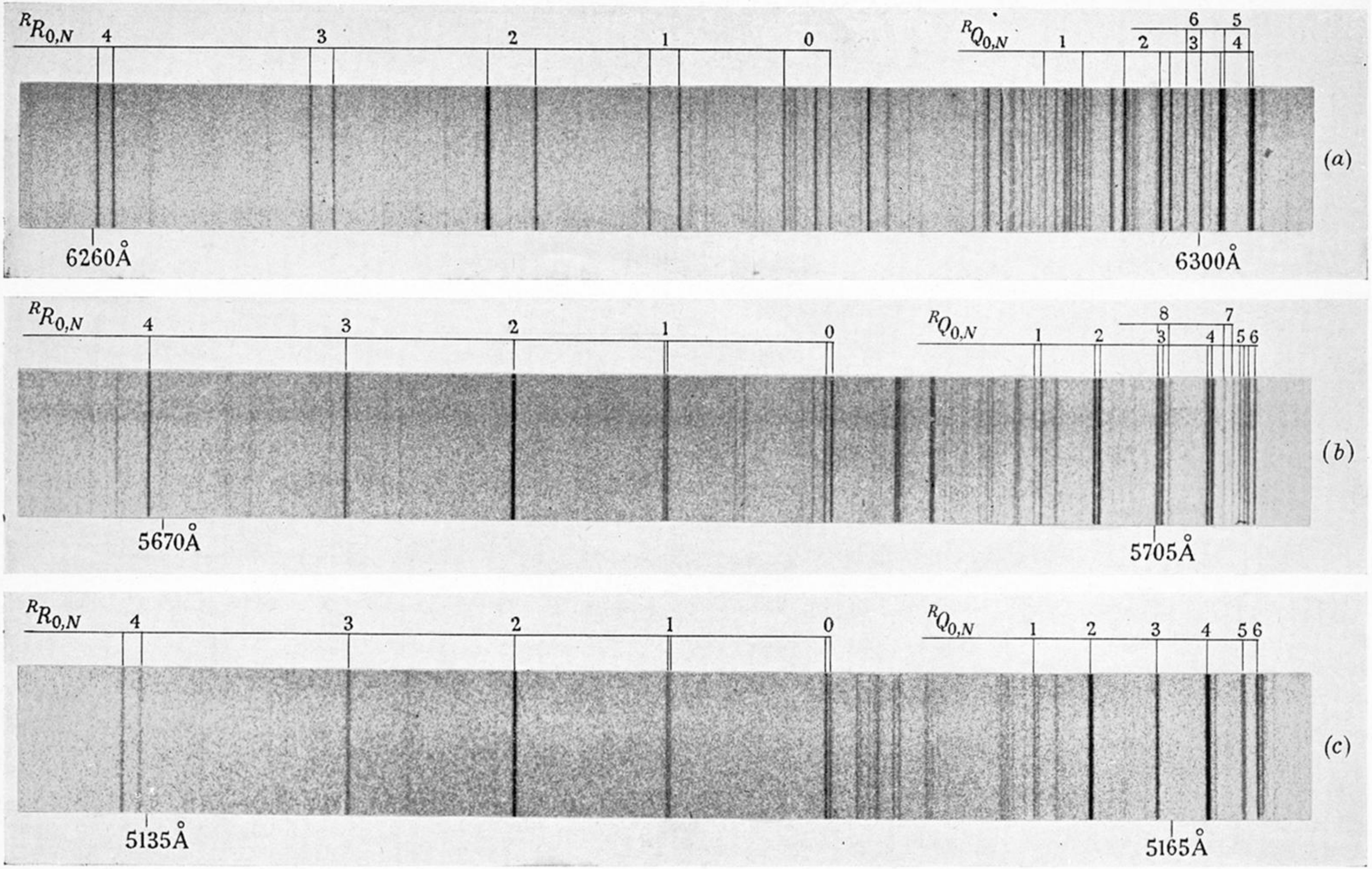

FIGURE 2. Comparison of the strong R and Q branches in the Π vibronic sub-bands of (a) the (0, 8, 0) $\leftarrow$ (0, 0, 0) band, (b) the (0, 10, 0) $\leftarrow$ (0, 0, 0) band and (c) the (0, 12, 0) $\leftarrow$ (0, 0, 0) band of NH_2. The decrease in spin splitting from (a) to (b) to (c) may be noted. A rotational perturbation may be seen in the $R(4)$ line in (c).

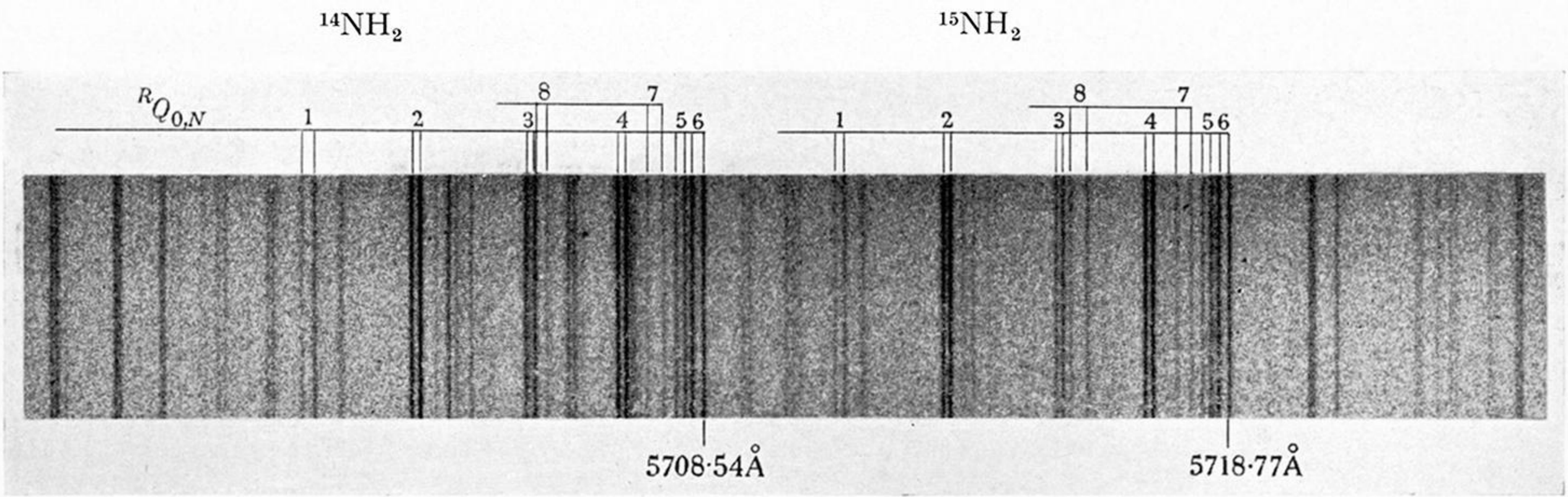

FIGURE 3. $^{14}NH_2$–$^{15}NH_2$ isotope shifts in the strong Q branch of the (0, 10, 0) ← (0, 0, 0) band of NH_2. This spectrogram was obtained by the flash photolysis of a mixture of $^{14}NH_3$ and $^{15}NH_3$ in roughly equal proportions.

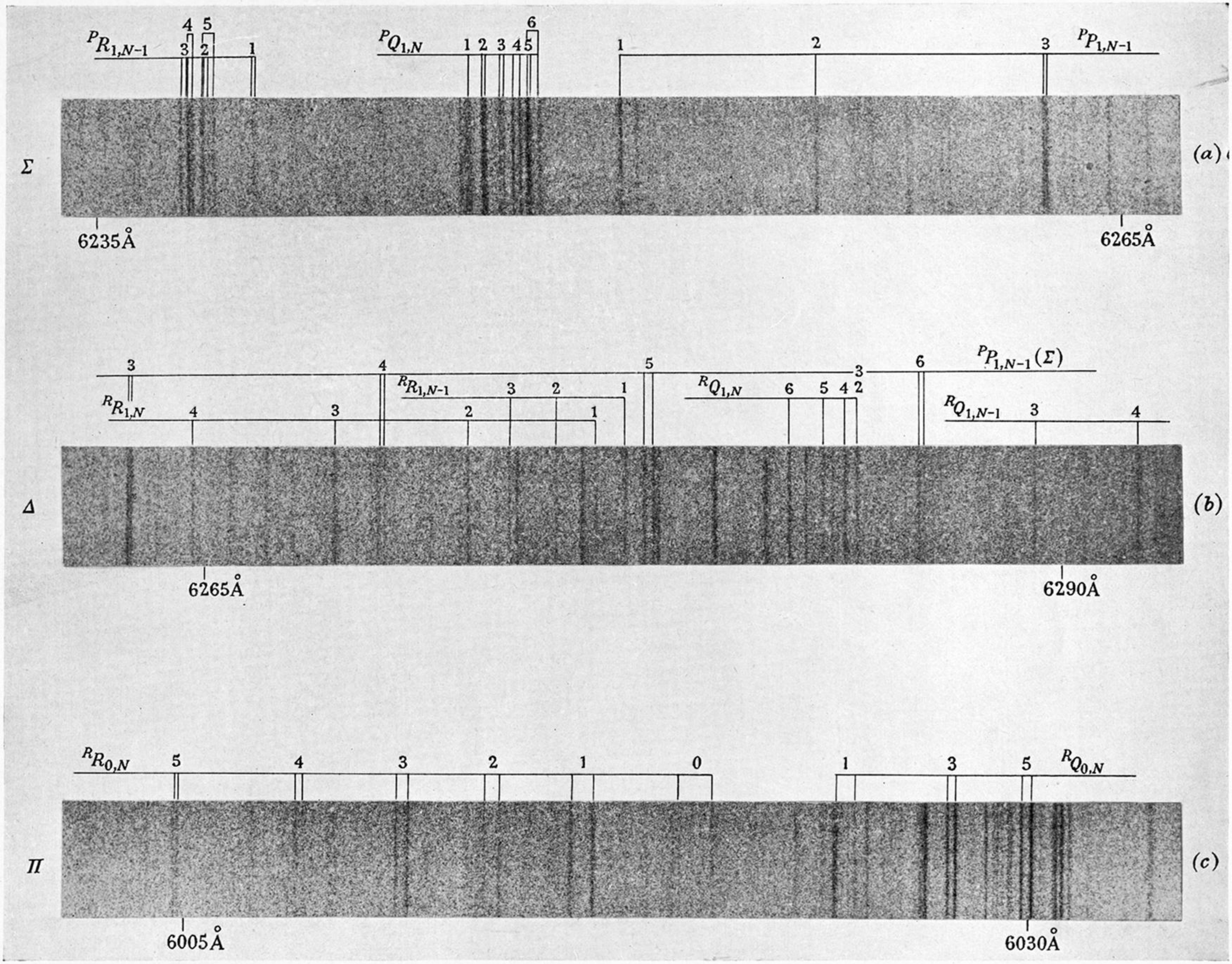

FIGURE 4. Rotational assignments for the strongest bands in the absorption spectrum of ND_2. In (*a*) the three branches of the Σ vibronic sub-band of the (0, 11, 0) ← (0, 0, 0) band are shown. In (*b*) the strongest *R* and *Q* branches of the Δ vibronic sub-band of the same band are given, together with the overlapping *P* branch from the Σ vibronic sub-band. In (*c*) the strong *R* and *Q* branches of the Π vibronic sub-band of the (0, 12, 0) ← (0, 0, 0) band are shown.